



National Institute of Technology, Rourkela

PROJECT REPORT ON

“LIQUEFACTION OF HELIUM AND NITROGEN WITH GM CRYOCOOLER”

A technical project report submitted in partial fulfillment of the requirement for the Degree of Master of Technology in Mechanical Engineering (Cryogenics and Vacuum Technology) under National Institute of Technology, Rourkela.

Submitted by:

Navneet Kumar Suman
Roll No. - 213ME5460

Under the guidance of

Mr. Anup Choudhury
Scientist F (External)
Cryogenics Group
IUAC, New Delhi

Prof. Sunil Kumar Sarangi
Director
National Institute of Technology, Rourkela



National Institute of Technology, Rourkela

DEPARTMENT OF MECHANICAL ENGINEERING

CERTIFICATE

This is to certify that the thesis entitled “LIQUEFACTION OF HELIUM AND NITROGEN WITH GM CRYOCOOLER”, being submitted by **Mr. Navneet Kumar Suman**, Roll No. 213ME5460 in the partial fulfillment of the requirements for the award of the Degree of Master of Technology (M.Tech) in Mechanical Engineering, is a research carried out by him at the department of mechanical engineering, National Institute of Technology Rourkela and Inter University Accelerator Center, New Delhi under our guidance and supervision. The result presented in this thesis has not been, to the best of my knowledge, submitted to any other university or institute for the award of any degree. The thesis in our opinion has reached the standards fulfilling the requirement for the award of the degree of by regulations of the Institute.

Mr. Anup Choudhury
Scientist F
Cryogenics Group
IUAC, New Delhi
Date:

Prof. Sunil Kumar Sarangi
Director
National Institute of Technology, Rourkela
Date:

CONTENTS

INDEX	Page No.
CERTIFICATE	i
CONTENTS	ii
ACKNOWLEDGEMENT	vi
ABSTRACT	vii
LIST OF FIGURES	ix
LIST OF TABLES	xiv
CHAPTER 1	
1. Introduction	2
1.1 Objective of the study	4
CHAPTER 2	
2. Literature review	6
2.1 History of Air/Nitrogen production	6
2.2 Idea behind cryocooler based Nitrogen Liquefaction System	6
2.3 History of Helium production and Liquefaction	7
2.4 Idea behind cryocooler based Helium Liquefaction System	8
CHAPTER 3	
3. Temperature sensor calibration	10
3.1 Introduction	10
3.2 Facility available for sensor calibration at IUAC New Delhi	10
3.3 Carbon composition resistor	10
3.3.1 Resistance temperature characteristic	11
3.3.2 Interpolation formulae and calibration curve	13
3.4 Silicon switching diode (Philips BAS16)	14
3.4.1 Voltage temperature characteristic	14

3.5 Diode 2	15
3.5.1 Voltage temperature characteristic	15
3.6 Sample holder	16
3.7 Experimental setup for calibration of sensors	17
CHAPTER 4	
4. Helium liquefaction by GM cryocooler	19
4.1 Principle used for Helium Liquefaction	19
4.2 Component used for helium liquefier	20
4.3 Description of principle components of Helium liquefier	20
4.3.1 Gifford-McMahon cryocooler	20
4.3.2 Practical Load Map of two-stage GM cryocooler	21
4.3.3 Experimental setup	21
4.3.4. Experimental Procedure	23
4.3.5 Practical Load Curve analysis	25
4.3.6 Temperature fluctuation of the cold head	29
4. 4 Cooling Curve (Temperature profile) for the study of precooling 31 effect in regenerator part of two-stage SRDK- 415D GM cryocooler	
4.4.1 Experimental Setup for generation of cooling curve	31
4.4.2 Experimental procedure for the generation of cooling curve 33	
4.4.3 Cooling curve by considering different type of Heaters	35
4.5 Mass flow controller and modular	38
4.6 Condenser	39

CHAPTER 5

5. Fabrication of dewar and Assembly	41
5.1 Fabrication of dewar	41
5.2 Assembly of the dewar	42
5.3 Assembly with GM cryocooler	43

CHAPTER 6

6. Experimental setup and results	45
6. 1 Experimental setup for Helium liquefaction system	45
6.2 Operation	46
6.3 Experimental Results	47
6.4 Calculation	49

CHAPTER 7

7. Nitrogen liquefaction with GM cryocooler	51
7.1 Principle used for Liquefaction of Nitrogen	51
7.2 Principle Components of Nitrogen Liquefier	52
7.2.1 Gifford-McMahon cryocooler	52
7.2.2 Dewar for Liquid Nitrogen	54
7.2.3 Rotary and Turbo molecular Pumping Station	54
7.2.4 Level sensor	55
7.2.5 Vacuum Gauge	55
7.2.6 Mass Flow Meter	55
7.2.7 Temperature Monitor and Temperature Sensor	55

7.2.8 Condenser	56
7.2.9 Filtration unit and Membrane Unit (N2 Separator)	56
7.2.9.1 Particulate filter	57
7.2.9.2 Coalescing filter	57
7.2.9.3 Carbon Adsorber	58
7.2.9.4 Membrane Unit (for nitrogen generation)	58
7.2.9.5 Working of Separation unit and Filtration Unit	60
CHAPTER 8	
8. Experimental results and its analysis	62
8.1 Experimental Setup for Nitrogen Liquefaction	62
8.2 Operation	64
8.3 Experimental Results	64
8.4 CFD Modeling for Nitrogen Precooling	73
CHAPTER 9	
9. Conclusion	80
REFERENCES	81

ACKNOWLEDGEMENT

*First of all, I would like to thank the Almighty, who was always there to guide me. I feel profoundly privileged to express my sincere gratitude and respect towards my supervisor **Prof. Sunil Kumar Sarangi**, Director, National Institute of Technology, Rourkela, and **Mr. Anup Choudhury** (Scientist F), Inter University Accelerator Centre, New Delhi, for their relentless help and constant guidance it would not have been possible for me to complete this work. **Prof. Sunil Kumar Sarangi** and **Mr. Anup Choudhury** are not only an erudite supervisor but also an icon of inspiration and encouragement in fulfilling my task. I owe a deep debt of gratitude to them. They have helped me from prologue to epilogue. I remain ever grateful to him.*

*I am indebted to **Dr. T. S. Datta** (Scientist H), **Mr. Soumen Kar** (Scientist F) of Inter University Accelerator Centre, New Delhi, who has inspired me days in and out with their advice and experience. My special thanks to **Mr. Manoj Kumar** (J.E), **Mr. Suresh Babu** (J.E), **Mr. Santosh Sahoo** (S.E) Cryogenics Group and **Ramcharan Meena** (Scientist C) Material Science Group of Inter University Accelerator Centre, New Delhi for their help and assisting my project and experiment. I am also thankful to Director and staff members of IUAC, New Delhi.*

*I would also like to convey my deep regards to **Prof. Sunil Kumar Sarangi**, Director, NIT Rourkela and **Dr. Ashok Kumar Satapathy**, Associate Professor Mechanical Department, NIT Rourkela for their indebted help and valuable suggestions for the accomplishment of my thesis work.*

*I extend my thanks to my friends especially **Mr. Vijay Soni** who worked with me in every difficulty which I have faced and his constant efforts and encouragement was the tremendous sources of inspiration.*

I express my sincere gratitude to all the Technician of cryogenic Group of IUAC New Delhi for their wonderful support.

*Parents are next to God and I would like to thank my parents **Shri Shiv Narayan Mandal** and **Shrimati Lakhi Devi** for their numerous sacrifices and ever increasing unconditional love and support.*

(Signature)

Navneet Kumar Suman

Roll No.-213ME5460

M.Tech, Mechanical Engineering

National Institute of Technology, Rourkela

ABSTRACT

The performance and reliability of cryocooler are continually improving. Consequently, the cryocooler based systems are also coming into the market and more frequently used by technical persons, scientists in their laboratory experiments or for commercial and space applications. The fundamental advantage of cryocooler is the small size of its cold head due to this it take little space and can be mounted on top of a Dewar, thus it helps in minimizing overall size of the cryocooler based setup. With this type of setup, it possible to fulfil the requirement of liquid helium and liquid nitrogen in laboratories where the consumption of liquid helium and liquid nitrogen is not in higher quantities. Dewar is used to store liquid cryogen, for production and storage purposes.

We have developed a small-scale helium liquefaction systems and a nitrogen liquefaction system separately that provide solutions for liquid helium usage in laboratories. The helium liquefaction systems use two-stage GM cryocooler with 1.5 W cooling power at 4.2 K (Sumitomo modelSRDK-415D with compressor CSW-71D, consuming 6.5 kW electrical power) to provide cooling and condensation at 4.2 K and the nitrogen liquefaction system use a Cryomech Single stage Gifford-Mcmahon cryocooler to provide cooling and condensation of nitrogen at 80 K with the refrigeration capacity of 266 W (Rated) at 80K. The cold head/liquefier resides inside of the neck of a dewar in both helium and nitrogen liquefaction system. The room temperature helium gas to be liquefied enters the neck of the dewar and is efficiently pre-cooled by cold head before being liquefied. The two-stage GM cryocooler with 1.5 W cooling power at 4.2 K (Sumitomo model SRDK-415D with compressor CSW-71D, consuming 6.5 kW electrical power), equipped with heat exchanger at 2nd stage for condensing the incoming precooled gas by exposing larger surface area. No additional cooling power of cryoliquids or additional Joule–Thomson stages was utilized in case of helium and nitrogen liquefaction system. Measurements of the pressure dependence of the liquefaction rate were performed in both case of liquefaction system. The assembly of two-stage Gifford -McMahon cryocooler with heat exchangers and helium liquefaction container is usually accomplished in helium liquefaction system and the assembly of single stage GM cryocooler with heat exchangers and nitrogen liquefaction container is usually accomplished in nitrogen liquefaction system. The pressure gauge has to be connected to the container in both type of liquefaction system to examine the oscillation that gives the liquefaction rate.

Also diodes are placed on the container to measure the temperature of helium and nitrogen at different stages in container.

A maximum value of 10.5 SLPM was obtained for 2.5-3 psi stabilized pressure of cryostat in case of helium liquefaction system. . In the event of nitrogen liquefaction system maximum liquefaction rate of 74.36 Ltr/day was obtained at 3psi stabilized pressure of cryostat in case of the experimental dewar. We have also varied the pressure from 3psi to 15 psi to increase the liquefaction rate in the event of nitrogen liquefaction system and production rate varies from 74.36 Ltr/day to 80 Ltr/day was obtained.

LIST OF FIGURES

Figure No.	Title	Page No.
CHAPTER 3		
Fig. 3.1:	Carbon Composition Resistor	11
Fig. 3.2:	Resistance versus Temperature Graph in Log ₁₀ scale	12
Fig. 3.3:	Resistance versus Temperature Graph at 0T and 8T Magnetic field in Log10 scale	12
Fig. 3.4:	Calibrated curve for carbon resistor sensor	13
Fig. 3.5:	Silicon Switching Diode (Philips BAS16)	14
Fig.3.6:	Voltage- Temperature graph of silicon diode	15
Fig.3.7:	Voltage- Temperature curve of Diode 2	15
Fig.3.8:	Sample holder	16
Fig.3.9:	Block diagram of experimental setup	17
Fig.3.10:	Actual experimental setup for calibration	17
CHAPTER 4		
Fig.4.1:	Photograph of the test cryostat integrated with double stage GM cryocooler	22
Fig.4.2:	Schematic diagram of test setup	22
Fig.4.3:	Internal view of the cryocooler-based test rig	23
Fig.4.4:	Block diagram of measurement system	23
Fig.4.5:	Refrigeration load curve for 2 nd stage with different load at 1 st stage of the SRDK-415D GM cryocooler	26
Fig.4.6:	Refrigeration load curve for 1 st stage with different load at 2 nd stage of the SRDK-415D GM cryocooler	26
Fig.4.7:	SRDK-415D GM cryocooler 2 nd stage refrigeration capacity versus temperature in the temperature range of 2.7K to 16K	27

Fig.4.8: The practical load map of SRDK-415D GM cryocooler	28
Fig.4.9: Commercially available load map of SRDK-415D GM cryocooler	28
Fig.4.10: Temperature fluctuation versus mass curve for the 2 nd stage of SRDK-415D GM cryocooler	29
Fig.4.11: Temperature fluctuation versus thermal conductance curve for the 2 nd stage of SRDK-415D GM cryocooler	30
Fig.4.12: ANSYS simulation of temperature fluctuation on the thermal mass for a given fluctuation on the 2 nd stage of SRDK-415D GM cryocooler	31
Fig.4.13: Schematic diagram of test setup	32
Fig.4.14: Block diagram for the test set up	33
Fig.4.15: Cooling curve of two stage 1.5W at 4.2K (SRDK-415D) GM cryocooler	34
Fig.4.16: Cooling curve of two stage 1.5W at 4.2K (SRDK-415D) GM cryocooler for 20W@ 1 st Stage and varying load @ 2 nd Stage	34
Fig.4.17: Schematic Diagram for test setup for thin rectangular heater	35
Fig.4.18: Cooling curve of two stage 1.5W at 4.2K (SRDK-415D) GM Cryocooler for heating at intermediate stage with 50Ω Heater	36
Fig.4.19: Schematic Diagram of test setup for wire heater	37
Fig.4.20: Cooling curve of two stage 1.5W at 4.2K (SRDK-415D) GM Cryocooler for heating at intermediate stage with Wire Heater	37
Fig.4.21: DFC digital mass flow controller and SDPROC Command Modules	39
Fig.4.22: Condenser	39

CHAPTER 5

Fig.5.1: Leak test of the cryogen reservoir assembly during cold shock with nitrogen and welding in flange of assembly	41
Fig.5.2: MLI wrapping and assembling of the dewar	42
Fig.5.3: Final assembly of setup with GM Cryocooler	43

CHAPTER 6

Fig.6.1: Actual Experimental setup	46
Fig.6.2: Position of temperature sensors	47
Fig.6.3: Cool down curve and flow rate during liquefaction of Helium	47
Fig.6.4: curve shows during operation vacuum increases, pressure of cylinder Decreases, total helium flow increases	48

CHAPTER 7

Fig.7.1: Cooling Capacity curve of AL300 GM cryocooler.	53
Fig.7.2: Condenser (HX2 with Long fins)	56
Fig.7.3: Actual complete setup of separation unit and Filtration unit	60

CHAPTER 8

Fig.8.1: Whole Experimental set up for Nitrogen liquefaction	63
Fig.8.2: Actual experimental set up for Nitrogen liquefaction	63
Fig.8.3: Temperature at different position of cryocooler and cryogenic reservoir vessel during liquefaction of nitrogen at 3 psi for inlet through neck port with HX2.	65
Fig.8.4: Cool down curve for neck inlet at operating pressure of 3 psi.	65

Fig.8.5: Temperature at different position of cryocooler and cryogenic reservoir vessel during liquefaction of nitrogen at 3 psi for inlet through neck port without HX2.	66
Fig.8.6: Cool down curve for neck inlet at operating pressure of 3 psi without condenser	67
Fig.8.7: Graph of mass flow at different pressure of vessel when nitrogen is taken from the atmosphere.	68
Fig.8.8: Graph of mass flow at different pressure of vessel when nitrogen is taken from atmosphere and vapour nitrogen from nitrogen dewar.	69
Fig.8.9: Bar graph of percentage increment in production rate in case of side inlet with heat exchanger from the base value (side inlet without heat exchanger).	69
Fig.8.10: Bar graph of percentage increment in production rate in case of neck inlet without heat exchanger from the base value (side inlet without heat exchanger).	70
Fig.8.11: Bar graph of percentage increment in production rate in case of neck inlet with heat exchanger from base value (side inlet without heat exchanger).	70
Fig.8.12: Sensors mounted on different position of the GM Cryocooler	71
Fig.8.13: Cryocooler temperature Profile at various positions for side inlet of nitrogen gas and for neck inlet of nitrogen gas	71
Fig.8.14: Cooling curve of AL300 GM Cryocooler in vacuum condition	74

Fig.8.15: Sensors position on GM Cryocooler for generating cooling curve in vacuum condition	74
Fig.8.16: Heat transfer coefficient graph at different position of Regenerator of AL300 GM Cryocooler	75
Fig.8.17: 2-D axisymmetric mesh model of cold head with Dewar neck for CFD analysis	75
Fig.8.18: Temperature contour and Temperature Profile of the nitrogen fluid through regenerator with 4mm annular gap	76
Fig.8.19: Flux report of the simulation for 4mm annular gap	76
Fig.8.20: Temperature contour and Temperature Profile of the nitrogen fluid through regenerator with 2mm annular gap.	78
Fig.8.21: Flux report of the simulation for 2 mm annular gap.	78

LIST OF TABLES

Table No.	Title	Page No.
CHAPTER 4		
4.1:	Different heat load applied at 1 st stage and second stage	25
4.2:	Production rate at different outlet temperature at the 2 nd stage of GM cryocooler	49
CHAPTER 8		
8.1:	Observation table for Run 1	66
8.2:	Observation table for Run 1	67
8.3:	Summarized data of Nitrogen Liquefaction	72
8.4:	Enthalpy and temperature for different geometry	78

CHAPTER 1

INTRODUCTION

CHAPTER 1

INTRODUCTION

The process of converting compressed gas into a liquid with the help of some mechanism is called liquefaction. Now a days almost all laboratories required liquid helium and liquid nitrogen for doing experiment in low temperature. Production and distribution of liquid helium and liquid nitrogen on large scale needs central facility to transport liquid in many cryostats. With the availability of small closed-cycle cryocooler, it is possible to liquefy helium and nitrogen nearby center or in cryostat also. This small closed cycle cryocooler allow their operation without support of cryogenic liquid. Development of efficient large-scale cryogenic liquefier, refrigerator and related processes has been one of the prime motivations for cryogenic community. The miniature source of cryogenic temperature could be achieved with the advent of Gifford Mac Mohan cryocooler (GM Cooler) in 1964 [1] and Pulse tube cryocooler (PT cooler) 1990 [2]. The most significant advantage of using the cryocooler is its user-friendly features like the minimum user interface in reaching the desired cold temperature and very fewer maintenance requirements. Because of the cyclical nature of pressure variation inside both the cryocooler the temperature at the cold end has inherent temperature fluctuations (~ 120 mK in GM cooler and ~ 100 mK in PT cooler). These devices are also vibration prone. Both the temperature and the vibration in the cryocooler are tolerable for experiments where only systemic behaviour is studied, but for precise transition measurement one must have a very stable source temperature. There is also the other issue of thermal gradient arising out of finite thermal conductivity of the medium. The best way to avoid the temperature and pressure fluctuations from the cryocooler is to use as a liquefier by using external condensing gas [3]. Apart from using this cryocooler as a liquefier they are being used as a recondenser as well, whereby the cold gas from the liquid is made to reach the cryocooler cold head with suitable condensation heat exchanger. The use of the cryocooler as liquefier and recondenser has led to many vital developments such as magnetic resonance imaging (MRI) cryostat with liquid helium (LHe), electron cyclotron resonance (ECR) cryostat (LHe), many types of nuclear detector cryostats with liquid argon, electrical energy storage device at the power distribution level SFCL using LN₂ etc.

A few other important issues are also helping the R&D in this field even more.

- (i) With the advent of using superconductivity in electrical application a lot of emphases is being put for the development SFCL, Cryogenic transformers, cryogenic energy storage all of them uses LN₂ /LHe in either liquefier or recondenser form.
- (ii) With no fresh source of helium being discovered for a long time and in face of increased usage of this precious natural resource for its vital role in health, mining and academic usage, the best way to preserve the same is to conserve helium gas.

The practical way to achieve the same is to use a cryocooler based recondensation process to recondense helium gas back to the respective dewar.

AT IUAC a successful attempt has been made in the development of table top nitrogen liquefier with the help of single stage GM cryocooler, and in the formulation of a helium liquefaction system using a 4.2K GM cryocooler. However an effort is being made to systematically study the liquefaction and recondensation process for both liquid nitrogen and liquid helium using GM cryocooler which will help to understand the fundamental heat transfer issues associated with the process of making efficient liquefaction and recondensation process in future.

A few particular points that will be considered for systematic studies are;

1. The role of inter-stage cooling where the gas undergoes precooling from the regenerator region of the cryocooler and its effect on the actual liquefaction capacity. Effect of natural convection vs. forced cooling and its impact on the heat transfer in the regenerator region will be studied.
2. Design issues involved with the condensation / recondensation heat exchanger leading to a better yield of liquid. The study will be focussed on the effect of using different conductive material with different geometries and its impact on the temperature difference across the heat exchanger.
3. The design of efficient cryostat dewars (liquid nitrogen and liquid helium) with GM cryocooler.

Two type of cryocoolers are mainly used for small scale liquefaction system and also available in the market, Pulse tube and Gifford-McMahon (GM) types. Without addition of cryo liquid and J-T valve maximum liquid helium production rate of 20 lit/day has been achieved using two-stage GM cryocooler in the setup. In case of nitrogen liquefaction system, we have obtained up to production rate of 80 lit./day at 15 psi stabilized pressure of experimental dewar and with the refrigeration capacity available at cold head. Dewar has 28 lit. capacity, which has been fabricated using the material available at IUAC.

1.2 Objective of Experiment

1. For liquefaction of helium, fabrication of an experimental cryostat and assembling cryocooler on it.
2. To achieve helium production rate of 20 Ltr/day.
3. To achieve necessary nitrogen production rate of > 75 Ltr/day.
4. To study the setup theoretically and analytically by assembling all data.
5. Optimize of production rate of setup with the help of condenser and precooling of gas in case of helium and nitrogen liquefaction separately.
6. CFD modelling of different situations in nitrogen liquefaction for better understanding of the system.

CHAPTER 2

LITERATURE REVIEW

CHAPTER 2

LITERATURE REVIEW

2.1 History of Air/Nitrogen Production

Carl Von Linde had liquefied air with the help of J-T Principle (J-T Valve) in 1872. In 1877 Paul Cailletel (Mining Engineer) obtained liquid oxygen fog with the help of compressing gas to 300 atm and precooling, then allow to expand the gas at the pressure of 1 atm. In 1877, a physicist Raoul Pictet used cascade system and successfully obtained liquid oxygen. K. Olszewski and Szymunt Von Wroblewski has liquefied oxygen and nitrogen in laboratory in 1883 at Cracow University. However, they have successfully condensed the gases first time but they are not able to kept the condensed gas in liquid form for long duration because of large amount of heat load coming from ambient condition in form of conduction, convection and radiation. This problem has been eliminated by James Dewar in 1892. James Dewar has discovered the vacuum jacket dewar for storing the liquid cryogen which eliminate the heat load problem mostly. Carl Von Linde had settled a Linde company in 1895, Now this company is the biggest company in the field of cryogenics.

In 1959, an advanced cooling system had been launched by McMahon and W.E. Gifford to develop compact and small cryogenic systems. The thermodynamic cycle on which this cooling system has been based, named as Gifford-McMahon cycle. The refrigerator system that runs on this cycle is known as Gifford-McMahon cryocooler. Now days, this system has been used for manufacturing of small-scale Helium and Nitrogen liquefaction systems, cooling MRI, NMR etc. due to its smaller size and efficient way of handling the heat load coming from atmospheric conditions makes more popular today.

2.2 Idea behind cryocooler based Nitrogen liquefaction system

Cryocooler based Nitrogen liquefaction plant has been preferred by small users whose daily consumption is 100 lit/day. Medium users mostly preferred Sterling or Linde plant to consume about 200 to 1000 lit/day. In laboratory like material science, Biomedical etc, the quantity of liquid nitrogen consumption is less than 100 lit/day. If the liquid nitrogen available for this laboratory will be nearby and can be easily transported and used would be the best option.

Thus cryocooler based liquefier is the best option in terms of reliability, space required, ease of maintenance, price for this type of laboratories.

Chao Wang of Cryomech Inc. had filed a patent on Gas Liquefier on Oct 10, 2007 and was accepted on Aug, 2009 using a Pulse tube refrigerator. In this liquefier he had placed cold head of P-T refrigerator inside the neck of dewar or cryostat to liquefy the gas into the dewar. This technique was invented for the purpose of providing liquid helium in small laboratories because most of helium liquefiers are larger in size and not suitable for small laboratories.

We have applied the principle used by Chao Wang for helium liquefier to design and develop a G-M cryocooler based nitrogen liquefier having liquefaction capacity more than 75 lit/ady. In this project we have studied the precooling effect given by the regenerator part of single-stage GM cryocooler and their temperature profile. We have also calculated the liquefaction rate enhanced with the help of condenser and precooling effect.

2.3 History of Helium Production and liquefaction

In the year 1868 Pierre Janssen, a French astronomer, studying solar spectrum during a solar eclipse in Guntur, A. P., discovers a spectral line unknown of the earth elements. Norman Lockyer, an astronomer and Edward Frankland, a chemist concurred with the existence of the new element and named the new element as Helium. In 1895 Sir William Ramsay at Royal Institute, London, identifies helium on Earth after examining the gases released on treating cleveite, a uranium containing mineral, with acid. In the year 1903 Helium discovered in the gas fields in Kansas, USA.

In the year 1908 Heike Kamerlingh Onnes of Leiden laboratories, Holland becomes the first to liquefy helium. Heike Kamerlingh Onnes used helium, given by Ramsay and that helium was extracted from the Monazite sand from Kerala coast sent by his brother Onno, an officer in the Dutch East India Company.

In 1972, First L-He production facility outside United States, set up in Poland. In the year 1993 L-He production expanded in Russia to supply to Western markets. In 1994, Algeria became a major source of helium production. In 2005, First helium extraction facility was established in Qatar, about the capacity of 20 million nm^3 per annum which was named as Phase I. In The year 2013 (Phase II) Qatar, the production rate increases to 38 million nm^3 per annum.

2.4 Idea behind cryocooler based Helium liquefaction system

Gifford and Longsworth in mid 1960s introduced a pulse Tube cooler for helium liquefaction system. After this invention essential improvement has been achieved in this refrigerator type of cooling in past decade. The modification done is: adding a buffer volume with the orifice valve at the warm end of P-T cooler which led to phase shift between pressure and velocity. This led to improvement in cooling performance. Thummes et al achieved a liquefaction rate of 127 ml/h with a pulse tube cooler which gives 170mW net cooling power at 4.2K. Matsubara achieved a temperature of 3.6 K with the help of three –stage pulse tube cooler which gives cooling power of 30mW at 4.2K. Thummes achieved the lowest temperature of 2.75K with the help of using two-stage pulse tube cooler. Wang, G. Thummes et al investigated a two-stage double inlet pulse tube cooler in 1996 for cooling below 4K. In the year 2012, Jost Diederichs, San Diego, CA (US) has made helium liquefier with pressure-controlled liquefaction chamber, with liquefaction rate of 22 lit/day. Recently in march 2015, Wuhan national high magnetic field centre in china has developed the helium liquefier with the help of five two-stage G-M cryocooler and achieved liquefaction rate of 83 lit/day.

CHAPTER 3

TEMPERATURE SENSOR CALIBRATION

CHAPTER 3

TEMPERATURE SENSOR CALIBRATION

3.1 Introduction

Some construction specifications and details dictate sensor accuracy and calibration tolerances and some projects have no direction other than “sensors ought to be calibrated.” Even if the user find the properly calibrated sensors for a particular measurement than the design aspect of the instrument may or may not satisfied with the shape and size of the sensors that led to error in measurement. We have not used Lakeshore silicon diode sensor(D-670, D-470) because of their larger in size even if their accuracy is good. In the regenerator zone of two-stage GM cryocooler, Lakeshore silicon diode sensor (D-670, D-470) has not proper contact with the wall of regenerator due to larger in size. Thus, we need to calibrate the smaller size sensor with the calibrated Lakeshore silicon diode sensor(D-670, D-470).We have calibrated 3 type of sensors to use in this experiment namely carbon composition resistors, Silicon Switching Diode(Philips BAS16), Diode 2.

3.2 Facility available for sensor calibration at IUAC New Delhi

For the calibration of sensors, a wet superconducting magnet system has been used which is available at IUAC New Delhi. In this magnet system at a time four sensors can be calibrated. In this setup that is shown in fig.9, We can calibrate the sensor by varying temperature as well as a magnetic field. We can change the temperature from 1.5K to 300K and the magnetic field from 1T-8T.This system contains liquid helium of 30 liters. This system is incorporated with the lab View for the calibration of sensors and for the purpose of finding materials property.

3.3 Carbon Composition Resistor

Carbon Resistors are widely used as secondary thermometers at low and very low temperature. These resistors are very sensitive, and their readings depend little on the magnetic field. These are widely used from 1K to 100K. Although they are less reproducible than resistance thermometer. They are inexpensive, and their small size is advantageous for mounting in cylindrical part near regenerator of GM Cryocooler. In Carbon Resistors

thermometer the resistance is dependent on current. So, for calibration and operation a constant current is required .we had supplied 100 μ A current for calibration of carbon resistors.

We have a wet superconducting magnet system in IUAC New Delhi, which has been manufactured by Oxford Instruments used for material property testing in a magnetic field as well as in very low temperature to room temperature. This system was used to calibrate carbon resistor. It has a probe on which samples have been placed and subject them to the magnetic field (varies up to 8Tesla) and very low temperature (varies from 1.5K to 300K) region. The probe base temperature is 1.5K then constantly heated up to 300K using temperature controller in the steps of 0.3K in Temperature range of 1.5-10K, 5K in Temperature range of 10K-100K, and step of 20 k in the Temperature range of 100K-300K. By measuring the resistance across the resistor at that temperature and with the help of measured data we get an R-T curve that can be feed into temperature monitor for that sensor. We have also repeated the calibration process starting from 300K and cooled up to 1.5K for the checking of repeatability of reading. At a time 4 carbon resistors had mounted on sample space in the probe with the help of GE varnish and Kapton tape, but at a time any two resistors had been calibrated. For the calibration 4-wire measuring technique had used to reduce the additional wire resistance error. For the minimization of Thermal voltage (V_{th}) current through current source meter had been sent twice and in a different direction but same value, so that positive and negative thermal voltage developed will cancel each other. Carbon resistor has been shown in fig.3.1

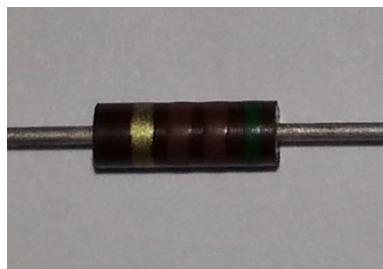


Fig.3.1: Carbon Composition Resistor

3.3.1 Resistance Temperature Characteristics

Fig.3.2 represents the resistance and temperature curve in log scale.

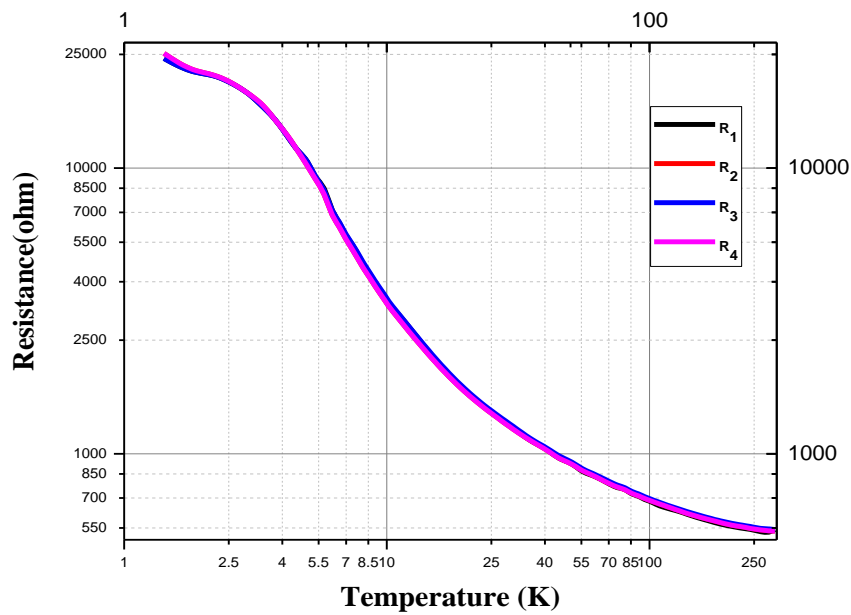


Fig.3.2: Resistance versus Temperature Graph in Log_{10} scale.

Fig.3.3 represents the Resistance-Temperature graph in the presence of magnetic field. From figure given in fig.3.3 we can say that there is a little variation of the result in a magnetic field with respect to the Non-magnetic field below 10K temperature.

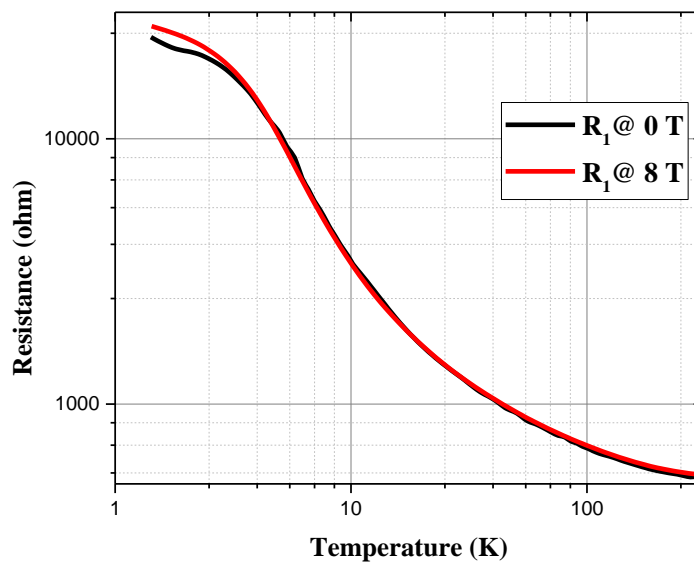


Fig.3.3: Resistance versus Temperature Graph at 0T and 8T
The magnetic field in Log_{10} scale

3.3.2 Interpolation formulae and calibration curve

Calibrated curve for calibrated carbon resistor has been obtained with the help of Origin Pro 8.0 software. The calibrated graph of Resistance-Temperature is shown in fig.3.4.

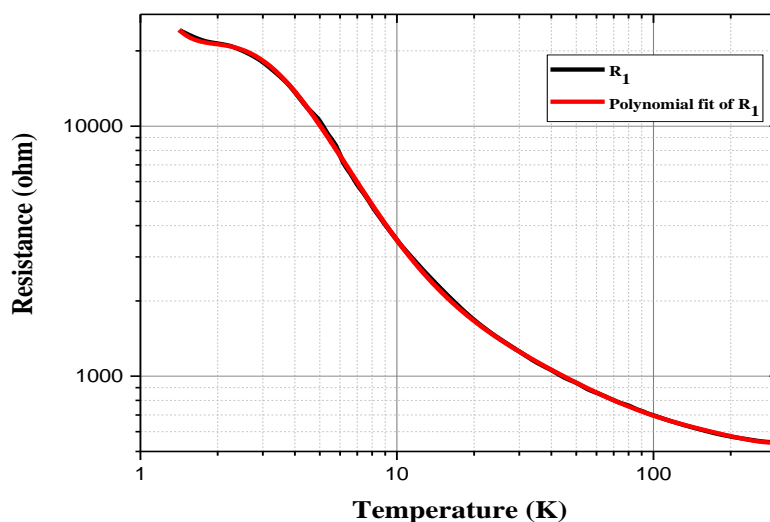


Fig.3.4: Calibrated curve for carbon resistor sensor

Empirical Equation of calibrated curve is given below.

$$R = \text{Intercept} + B1 \cdot T^1 + B2 \cdot T^2 + B3 \cdot T^3 + B4 \cdot T^4 + B5 \cdot T^5 + B6 \cdot T^6 + B7 \cdot T^7 + B8 \cdot T^8 + B9 \cdot T^9$$

The value of constant of the empirical equation is given in table below.

Intercept	4.80902
B1	-5.43996
B2	24.10037
B3	-51.28508
B4	52.97219
B5	-27.63567
B6	5.73273
B7	0.78321
B8	-0.56521
B9	0.07251

3.4 Silicon Switching Diode (Philips BAS16)

Silicon Switching Diode is mostly used in high-speed switching in hybrid and thick and thin film circuits. In silicon diode sensor, forward voltage is current dependent, therefore, this diode has to be operated at constant current for their calibration. Calibration is done in the same setup that has discussed for carbon resistor, but here $10\mu\text{A}$ current has been passed through silicon diode. In this case also the probe base temperature is 1.5K then constantly heated up to 300K using temperature controller in the steps of 0.3K in Temperature range of 1.5-10K, 5K in Temperature range of 10K-100K, and step of 20 k in the Temperature range of 100K-300K. By measuring the voltage across the diode at that temperature we get a V-T curve that can be feed into temperature monitor for that diode sensor. The Same procedure has been followed for diode calibration as mention above. The silicon diode picture has been shown in Fig.3.5.

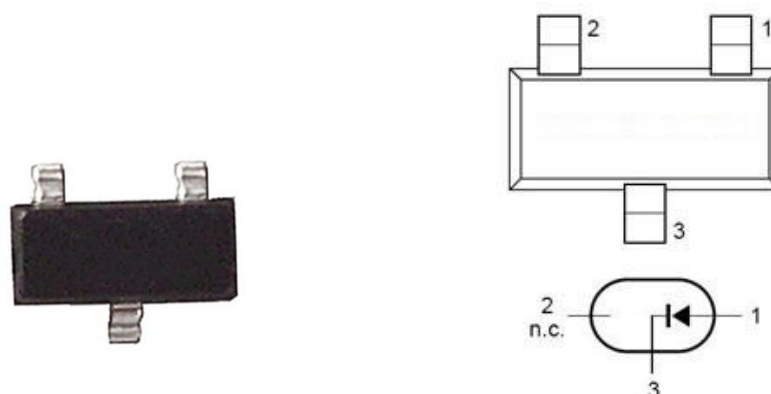


Figure 3.5: Silicon Switching Diode (Philips BAS16)

3.4.1 Voltage Temperature Characteristics

The Voltage- Temperature graph has been shown in fig.3.6. From 300K to 15 K silicon diode shows smooth curve but after 15K it shows some fluctuation that is not shown in graph below. This curve shows linear behaviour in temperature between 30K-300K .Below 30K the voltage of the diode sensor rises sharply. This diode below 10K does not shows continuous curve and curve follows the zigzag path. Since, below 10K diode shows irregular pattern in curve so it is not used for the temperature measurement below 10K but can be used for temperature measurement above 10K.

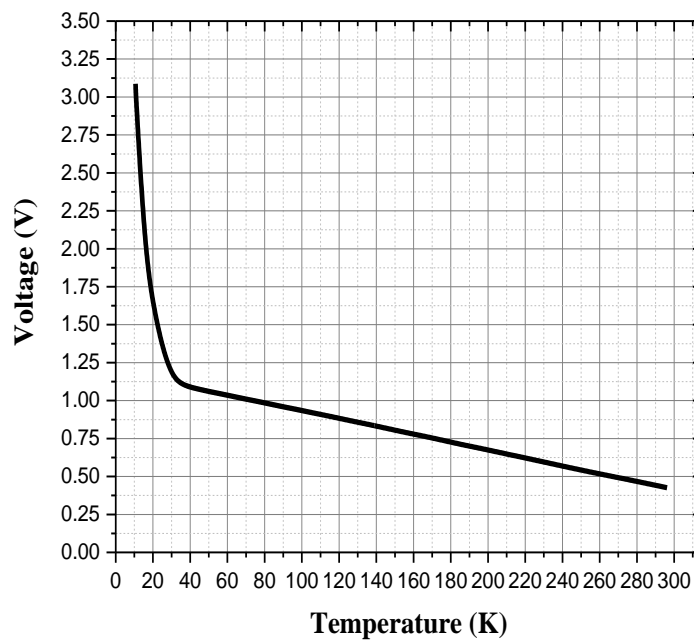


Fig.3.6: Voltage- Temperature graph of silicon diode

3. Diode 2

3.5.1 Voltage Temperature Characteristics

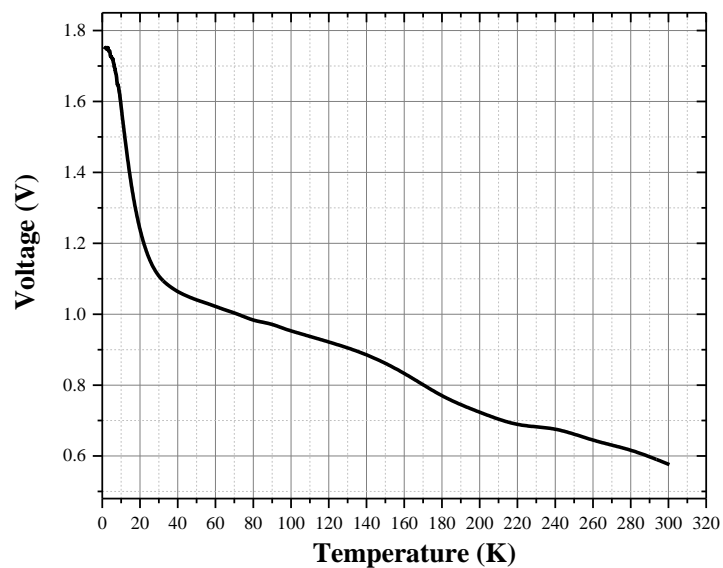


Fig.3.7: Voltage- Temperature curve of Diode 2.

3.6 Sample Holder

The sample holder for wet superconducting magnet system had also been manufactured in IUAC New Delhi so that the probe weight should be less and carry the minimum load at room temperature. The design of sample holder or probe has been done in solid works 2013 version. Fig.3.8 shows the picture of the sample holder and how the sample has mounted on it.

Material used for sample holder are-

- Stainless Steel(SS304)
- Copper
- Stainless Tube

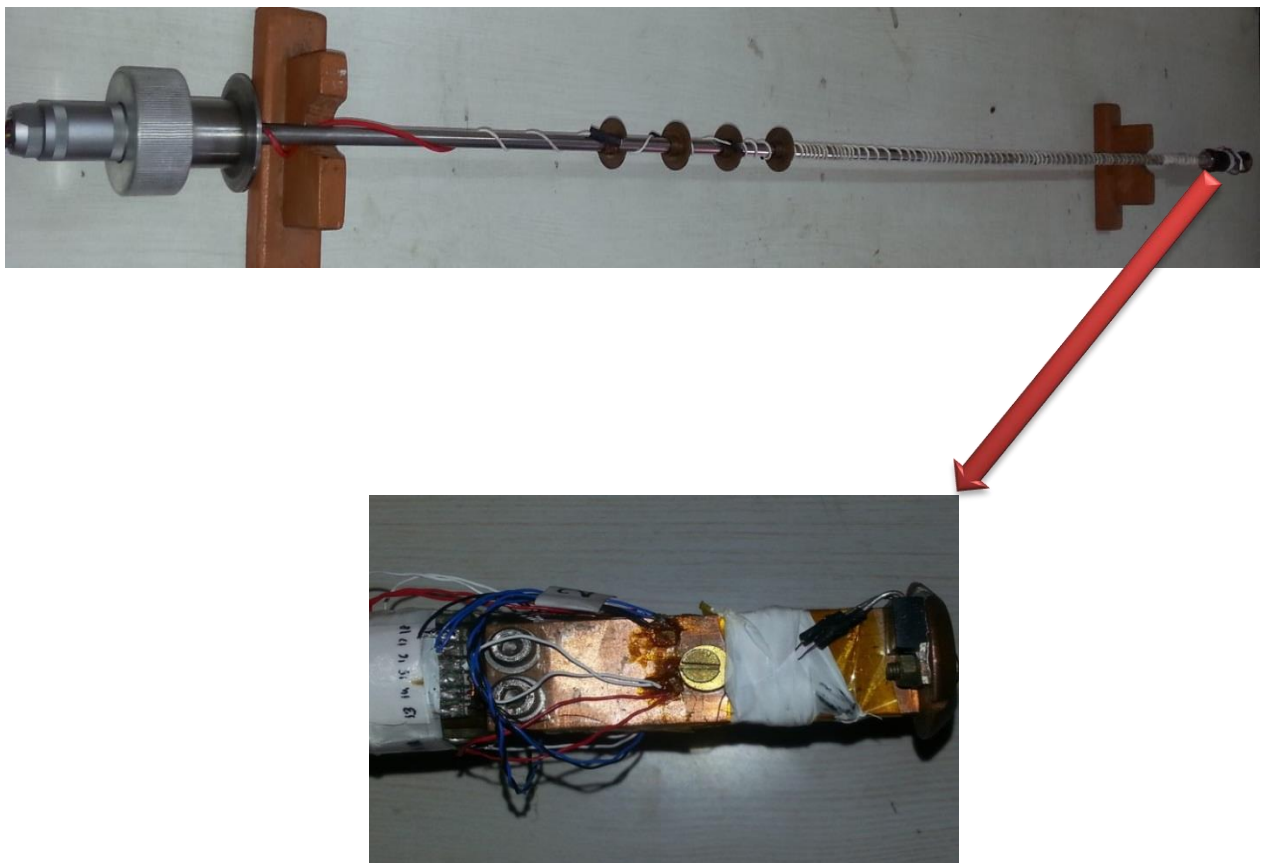


Fig.3.8: Sample holder

3.7 Experimental Setup for Calibration of sensors

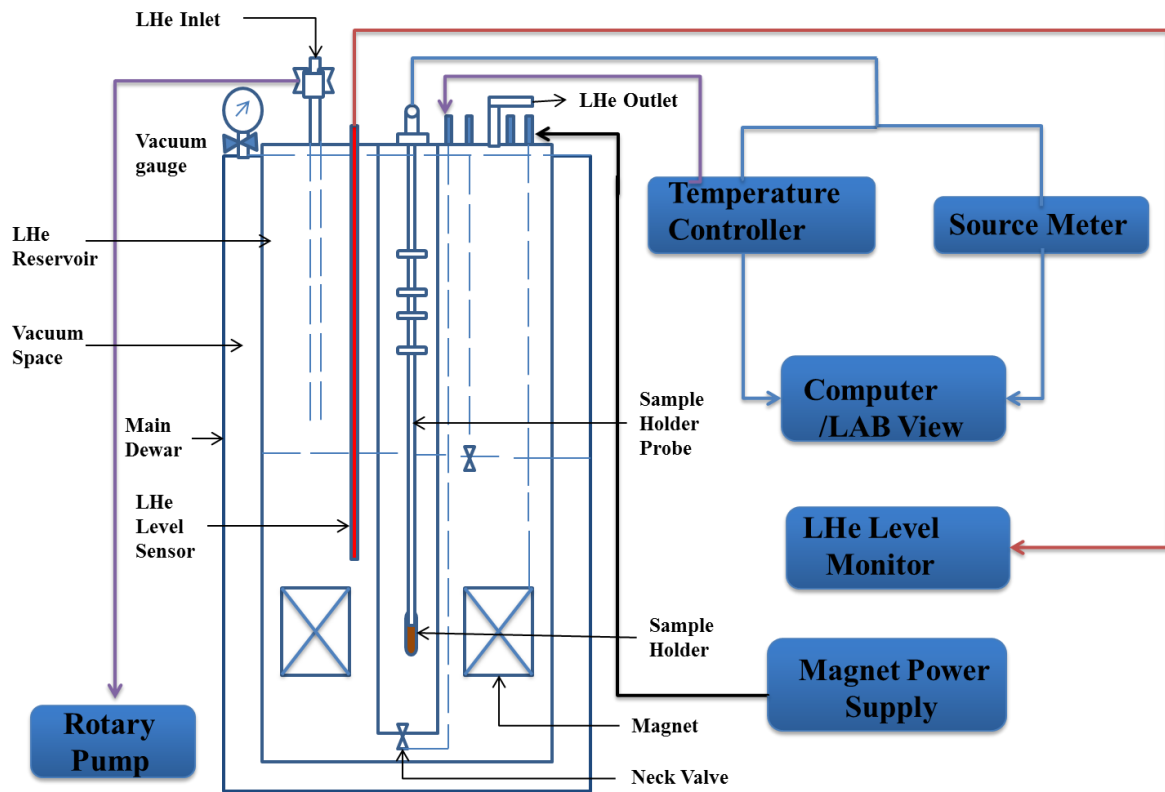


Fig.3.9: Block diagram of experimental setup



Fig.3.10: Actual experimental setup for calibration.

CHAPTER 4
HELIUM LIQUEFACTION
WITH GM CRYOCOOLER

CHAPTER 4

HELIUM LIQUEFACTION WITH GM CRYOCOOLER

4.1 Principle used for Helium Liquefaction

For the production of liquid helium, we have taken helium gas from helium gas cylinder, then cool it down with the help of two-stage GM cryocooler to 4.2 K for condensation. Along with the Condensation of liquid helium, storage of liquid helium is also an important problem; Because helium stays liquid at 4.2 K, by exposing to atmospheric conditions liquid helium will not stay in liquid state for long time. Cryogenic storage tanks and Dewars have been designed and manufactured to store liquid helium in it. These vessels are vacuum jacketed (double walled) to separate the vessel which is carrying the liquid helium from atmospheric conditions. The space between them is evacuated to reduce convection loads, and 35 layers of multi-layer insulation have been utilized to diminish radiation load coming from outer vacuum vessel at 300K to inner cryogenic reservoir at 4.2K. In this project a commercially available two-stage GM cryocooler with 1.5 W cooling power at 4.2 K (Sumitomo model SRDK-415D with compressor CSW-71D, consuming 6.5 kW electrical power) has been used to provide cooling and condensation at 4.2 K. The cryocooler head is mounted into the highest point of the dewar and it reaches out down into the neck of dewar with the end goal of cooling the helium gas entering the dewar to 4.2K. Helium gas liquefies when it comes in contact with the cold head heat exchanger. The condensed helium trickles off the heat exchanger down into the dewar. This procedure would normally bring down the pressure inside the dewar but the pressure controller permits more helium gas to enter the dewar to keep the pressure at the preset level. The stream rate of the helium gas into dewar is controlled by the rate of liquefaction inside the dewar. We have achieved a production rate of 20 Litre/day at 2.5-3 psi in an experimental with 3 Litres capacity. We have used hollow structure made of 1 mm thick G10/Nylon material to guide the helium along the surface of both the stages of the cryocooler.

4.2 Component used for helium liquefier

The main component of this setup is;

1. Two Stage 1.5W at 4.2K (SRDK-415D) GM Cryocooler
2. 0.5mm thick SS Tubes
3. Copper block
4. 1 mm thick G10/nylon pipe
5. Heat Exchanger (Condenser)
6. Compressor
7. Helium Flex Lines
8. Dewar
9. Pressure Regulator
10. Mass flow controller and modular

4.3 Description of principle components of Helium Liquefier

4.3.1 Gifford-McMahon cryocooler

Introduction

Gifford–McMahon (GM) cryocoolers were first developed in 1960 which was based on closed loop helium refrigeration cycles. The use in 1990 of regenerators made with rare earth materials with high heat capacities in the range of 4–20 K allowed the GM cryocooler to achieve temperatures of 4.2 K. The Gifford –McMahon (GM) is a valved system regenerative type of cryocooler. This valve mechanism is used to generate the pressure variation or the pressure pulse. The sequential opening and closing of these valves generate the required pressure variation or the pressure pulse. Commercially available cryocoolers have rotary valves to control or regulate the flow of the working medium.

The basic components of any GM cryocooler are as follows-

1. Helium compressor –scroll/reciprocating type.
2. Flex lines –HP line, LP line.
3. Regenerator(s) and Displacer(s).
4. Valve mechanism –rotary, solenoid, poppet.
5. Cooling arrangements –Air or water cooled

4.3.2 Practical Load Map of two-stage GM cryocooler

A two stage 1.5W at 4.2K (SRDK-415D) GM Cryocooler has been used for the liquefaction of Helium. The commercial load map of this cryocooler is mainly based on some limited discrete points which most of the time is not sufficient for detailed thermal analysis of any cryocooler based system. We have to do sometimes interpolation to get particular value. Hence, to analyse the thermal behaviour of any cryocooler based systems, it is necessary to know the continuous load curves of the cryocooler along with its detailed load map. We have generated full scaled thermal load map that will help in analysing any cryocooler based systems.

4.3.3 Experimental setup

An industrial type, two stage 1.5W at 4.2K (SRDK-415D) GM Cryocooler is integrated with a small cryostat test rig. The test cryostat is shown in fig.4.1. The first stage of the cryocooler is attached with the thermal radiation shield made of copper. Four calibrated silicon diode temperature sensors (DT-670; Lakeshore) namely T1, T2, T3 and T4 have been attached respectively with 2nd stage cold head, sample plate, 1st stage cold head and top lid of the thermal shield as shown in Fig.4.2. Two heaters (H1, H2) have been mounted on each stage of cryocooler as shown in Fig.10. Few layers of multi-layer insulation have been provided over the each stage of cryocooler to reduce the radiation heat flow to the cold heads. Fig.4.3 shows the internal view of the test rig. A block diagram for the test set up is shown in the Fig.4.4. We have used an 8-channel temperature monitor (Lakeshore, model-218) for temperature measurement and two source meters (Agilent and Kepco) have been used for powering the heaters.



Fig.4.1: Photograph of the test cryostat integrated with double stage GM cryocooler.

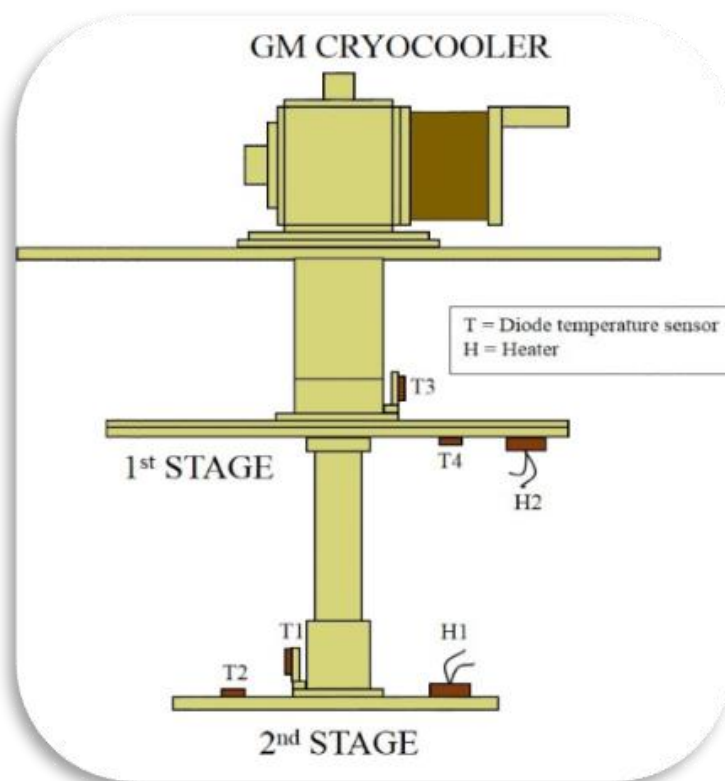


Fig.4.2: Schematic diagram of the test setup.



Fig.4.3: Internal view of the cryocooler-based test rig.

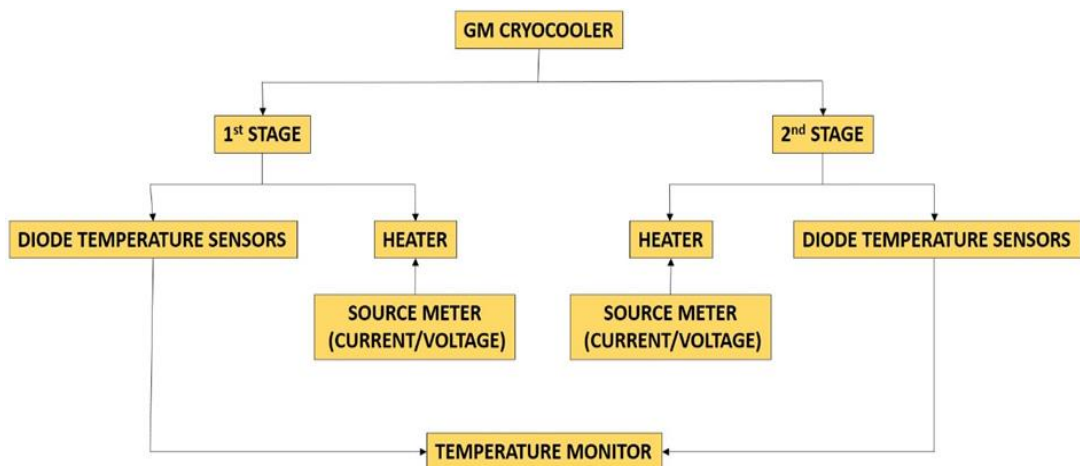


Fig.4.4: Block diagram of the measurement system.

4.3.4. Experimental Procedure

At first, integration of the whole system was completed. A turbo molecular pump based pumping system has been attached to the cryostat to generate the vacuum. To measure the vacuum level, a Penning gauge (Pfeiffer Vacuum) has been attached with the cryostat. A dual gauge display (Pfeiffer Vacuum) has been used to monitor the vacuum. When the vacuum of the cryostat reached to $10\text{E-}04$ mbar level, the GM cryocooler has been started for cooling down the cryostat. The vacuum of the cryostat improved to $10\text{E-}08$ mbar due to the cryopumping by the cryocooler. At the steady state condition, the temperature of the 2nd stage of the cryocooler reached to 2.7 K. The steady state temperatures of sample plate (T2), 1st stage cold head (T3) and top lid of the thermal shield (T4) respectively are 2.65 K, 28.98 K, 29.5 K. These steady state temperatures correspond to the finite static heat load that is not zero. The temperature corresponding to zero load was estimated by interpolating the load curve that will be discussed later.

Initially, the temperature of the 1st stage is raised to a next higher value of temperature by giving known amount of heat (Q2) using H2 heater. Once the temperatures are stabilized, H1 heater connected at the sample plate has been powered with a known amount of heat (Q1). The temperature of the 2nd stage of the cold head would start rising. It would take some time to reach an equilibrium temperature corresponding to the Q1 heat. Once an equilibrium temperature corresponding to Q1 heat is reached, next value of known heat (Q1') has been given to the H1 heater and left for thermal stabilization. Once the temperatures are stabilized corresponding Q1' heat, increase the heat to the next value and so on. The power on the H1 heater is given in steps of 0.1W, 0.25W, 0.5W, 1W, 1.5W respectively.

When heat applied to the 2nd stage, the temperature rises sharply but after few interval of time it gets stable. The steady state temperatures corresponding to each value of heat Q1 have been noted down. Hence, a load curve of 2nd stage refrigeration capacity corresponding to the temperature has been generated for a particular heat load (Q2) at the 1st stage. A similar procedure has been repeated for different values of heat load (Q2) at the 1st stage. The values of Q2 have been varied in steps of 7.5W, 12.5W, 17.5W, 22.5W, 27.5W, 32.5W, 37.5W, 47.5W respectively. When the heat (Q2) has been given to the 1st stage of the cryocooler then the cryocooler take longer time to reach steady state because of higher heat load at 1st stage.

Similarly, the heat loads to the 1st stage have been varied for a constant heat at 2nd stage cold. The load curve for the 1st stage has been generated for different values of heat at the 2nd stage. The Tabular form of heat load applied on 1st stage and 2nd stage of GM cryocooler is given below.

Tabl.4.1: Different heat load applied at 1st stage and second stage

Heat given on 1 st stage of Cryocooler(Q2)	7.5W	12.5W	17.5W	22.5W	27.5W	32.5W	37.5W	47.5W
Heat gave on 2 nd stage of Cryocooler(Q1)	0.1W	0.25W	0.5W	0.75W	1W	1.5W		

4.3.5 Practical Load Curve analysis

Refrigeration load curves for 2nd stage cold head at different loads of 1st stage have been shown in Fig.4.5. It shows that the refrigeration capacity of 2nd stage corresponding to a particular temperature increases at the higher heat load at the 1st stage. The refrigeration load of the 2nd stage at 3.75K is 0.87W approximately at zero load at the 1st stage. At 3.75K, the refrigeration load at 2nd stage increases to 1.26W when the load at the 1st stage increases to 47.5W as shown in Fig.13. It has been observed during the measurement that, at the higher heat input, it takes a longer time to reach the equilibrium. For each reading, we have given sufficient time to stable.

Fig.4.6 shows the refrigeration load curves for 2nd stage cold head for different heat loads at 2nd stage cold head. It shows that the refrigeration capacity of 1st stage corresponding to a particular temperature decreases at the higher heat load at the 2nd stage. The refrigeration load of the 1st stage at 40K is 25.6W approximately at zero load at 2nd stage. The refrigeration load at 2nd stage decreases to 22.4W when the load at the 2nd stage increases to 1.5W as shown in Fig.14.

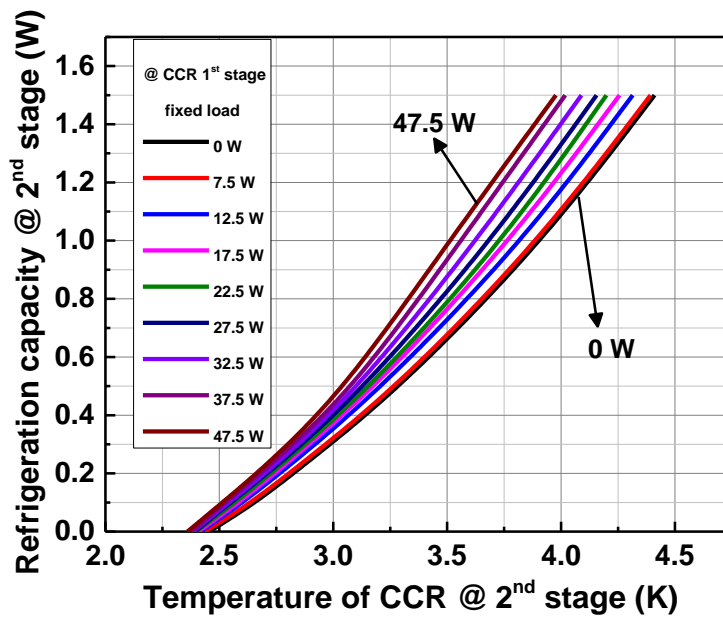


Fig 4.5: Refrigeration load curve for 2nd stage with different load at 1st stage of the SRDK-415D GM cryocooler.

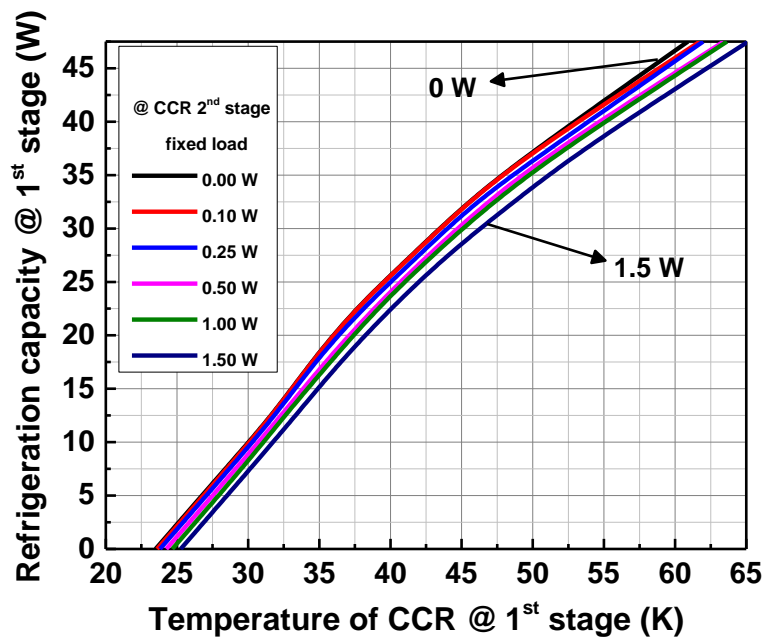


Fig.4.6: Refrigeration load curve for 1st stage with different load at 2nd stage of the SRDK-415D GM cryocooler

Fig.4.7 shows the refrigeration load curve for the 2nd stage up to the temperature of 16K. In this measurement, the Q1 heat at the 2nd stage of the cryocooler has been varied. The temperature of the 1st stage changes with the change in the 2nd stage temperature. This curve would also help in the estimation of the energy dumped into NbTi magnet system after quenching. It would also help to estimate the post-quench recovery of conduction cooled NbTi magnet.

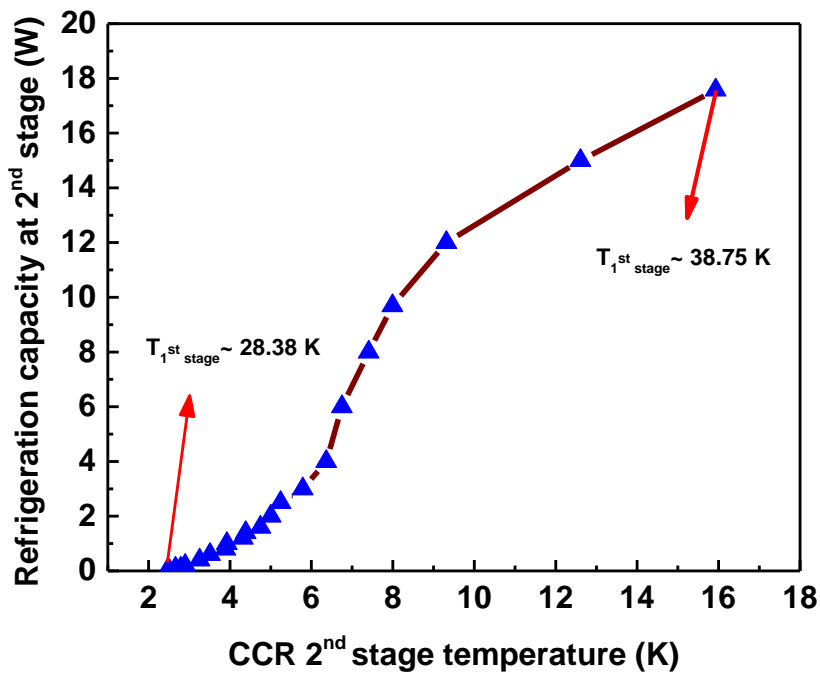


Fig.4.7 SRDK-415D GM cryocooler 2nd stage refrigeration capacity versus temperature in the temperature range of 2.7K to 16K.

Using, the load curves shown in Fig.4.5 and Fig.4.6, the practical load map of SRDK-415D GM cryocooler has been generated as shown in Fig.4.8. In Fig.4.8, X-axis represents the temperature of 1st stage and Y-axis represents the temperature of the 2nd stage. These practical load curves (Fig.4.5, Fig.4.6, and Fig.4.7) and load map (Fig.4.8) cover multiple number of thermal operating points of GM cryocooler which is generally not given in commercially available load map as shown in Fig.4.9.

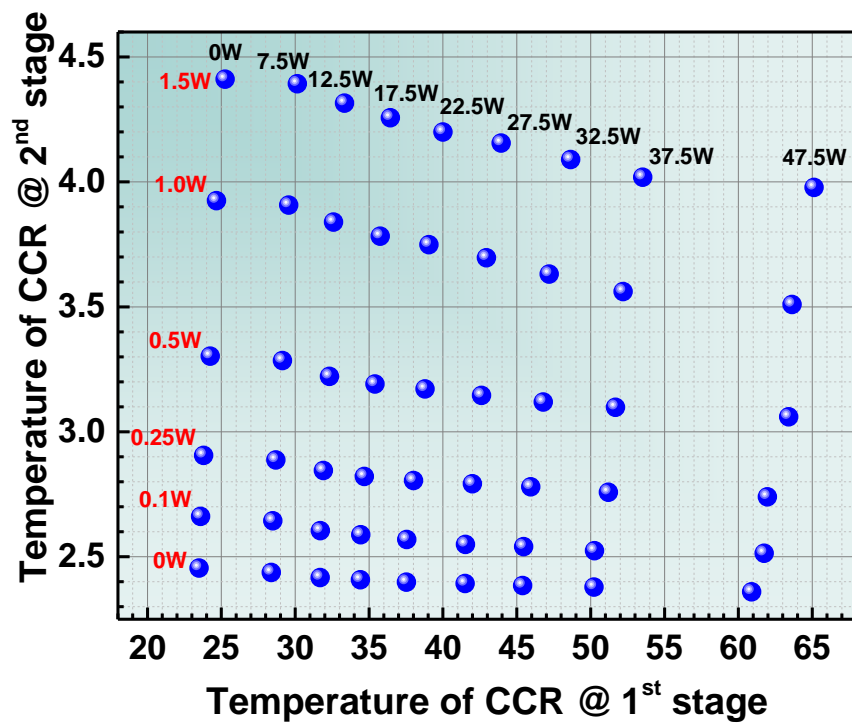


Fig.4.8.The Practical load map of SRDK-415D GM cryocooler.

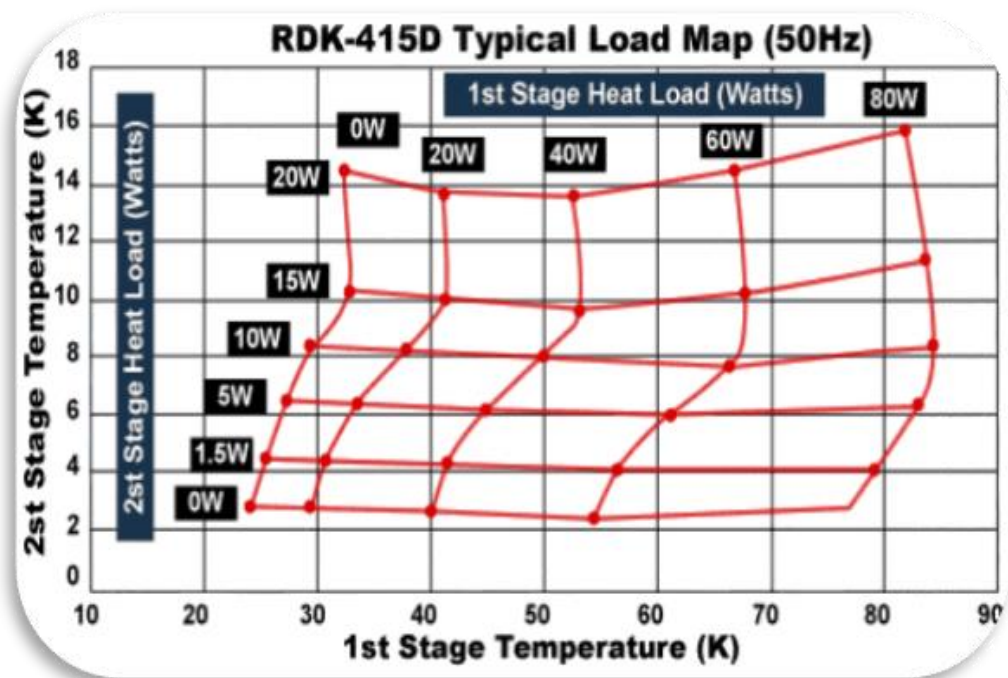


Fig.4.9: Commercially available load of SRDK- 415D GM cryocooler map.

4.3.6 Temperature fluctuation of the cold head

There is an inherent fluctuation of the temperature of both cold heads of GM cryocooler. The temperature fluctuation at the cold head generates an error in estimation of the heat load especially at the 2nd stage where the amplitude of fluctuation is more. Temperature of the 2nd stage the cold head of the GM cryocooler (SRDK-415) fluctuate as a result of reciprocating process that comprise the GM cycle. The peak to peak fluctuation can be as high as 400-500mK. For precession measurement, the fluctuation needs to be reduced. The temperature fluctuation would mainly depend on two parameters that are a thermal mass of sample, thermal conductance between the sample and 2nd stage of the cryocooler. To show the relationship, analysis of the fluctuation of temperature and their dependency on another parameter has been done in ANSYS 14.5 simulation software.

At first, for a constant mass of 2.5 kg attached at the 2nd stage of the cryocooler, the temperature fluctuation has been matched in ANSYS software with the actual experimental temperature fluctuation. After that by keeping the same temperature fluctuation and other parameters constant, we had varied the different mass value. Fig.4.10 shows the temperature fluctuation versus mass curve for the 2nd stage of SRDK-415D GM cryocooler. It shows that for a constant heat load as we increase the mass of plate, which we mounted to the 2nd stage cold head of the cryocooler, the temperature fluctuation at the mounted plate decreases, and shows asymptotic characteristic at higher mass values.

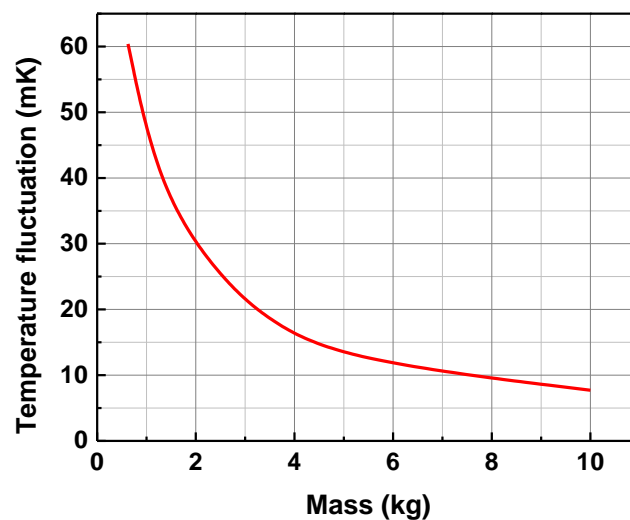


Fig.4.10: Temperature fluctuation versus mass curve for the 2nd stage of SRDK-415D GM cryocooler

For a constant mass of 2.5kg, constant temperature fluctuation and constant maximum temperature limit, a graph has been drawn by varying thermal conductance value in ANSYS. Fig.4.11 shows the ANSYS simulation of temperature fluctuation versus the thermal conductance curve. This curve shows that for a constant heat load, if the thermal conductance between the sample and the cold head is increased the amplitude of temperature fluctuation would increase.

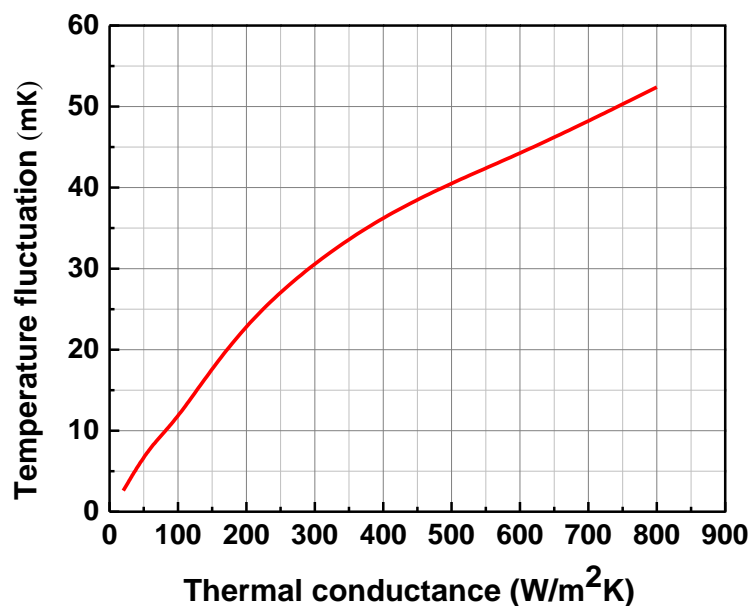


Fig.4.11: Temperature fluctuation versus thermal conductance curve for the 2nd stage of SRDK-415D GM cryocooler

Fig.4.12 shows the ANSYS simulation of temperature fluctuation on the thermal mass for a given fluctuation on the 2nd stage of SRDK-415D GM cryocooler. The input temperature fluctuation is in the range of 2.398K to 2.497 K and the fluctuation range is ± 50 mK. The output fluctuation has been reduced to ± 12 mK. The output temperature fluctuation is in the range of 2.6149K TO 2.5919 K. This result is obtained for the mass of 2.5 kg.

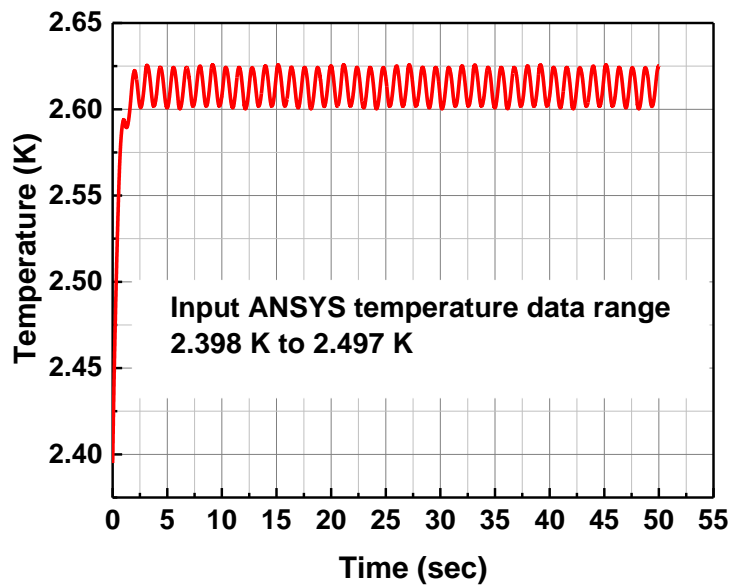


Fig.4.12: ANSYS simulation of temperature fluctuation on the thermal mass for a given fluctuation on the 2nd stage of SRDK-415D GM cryocooler

4. 4 Cooling Curve (Temperature profile) for the study of precooling effect in regenerator part of two-stage SRDK- 415D GM cryocooler

For the liquefaction of helium precooling effect in regenerator part of GM cryocooler plays very important role, which can be also shown in the above calculation. The cooling curve at different load has been drawn experimentally to estimate the precooling effect in regenerator part of GM cryocooler. For the generation of cooling curve, different experimental setup and procedure have been followed.

4.4.1 Experimental Setup for generation of cooling curve

An industrial type, two stage 1.5W at 4.2K (SRDK-415D) GM Cryocooler is integrated with a small cryostat test rig. The cryostat is shown in fig.9 .The cryostat is leak proof and actively checked with the mass spectrometer leak detector. The first stage of the cryocooler is attached with the thermal radiation shield made of copper. Two calibrated silicon diode temperature sensors (DT-670; Lakeshore) namely T1 and T2 have been attached respectively with 1st stage cold head and 2nd stage cold head as shown in Fig.21.Two heaters (H1, H2)

have been mounted on each stage of cryocooler as shown in Fig-21. Few layers of multi-layer insulation have been provided over the each stage of cryocooler to reduce the radiation heat flow to the cold heads. Five calibrated carbon resistor sensors (each 540 ohm, Allen-Bradley) namely S1, S2,S3,S4, and S5 have been attached in regenerator part at equal distance as shown in fig.4.13.All five sensors are connected in series with help D-connector. A block diagram for the test set up is shown in the Fig.4.14. Carbon resistor has been used as temperature sensor because of small in size and their accuracy at low temperature.

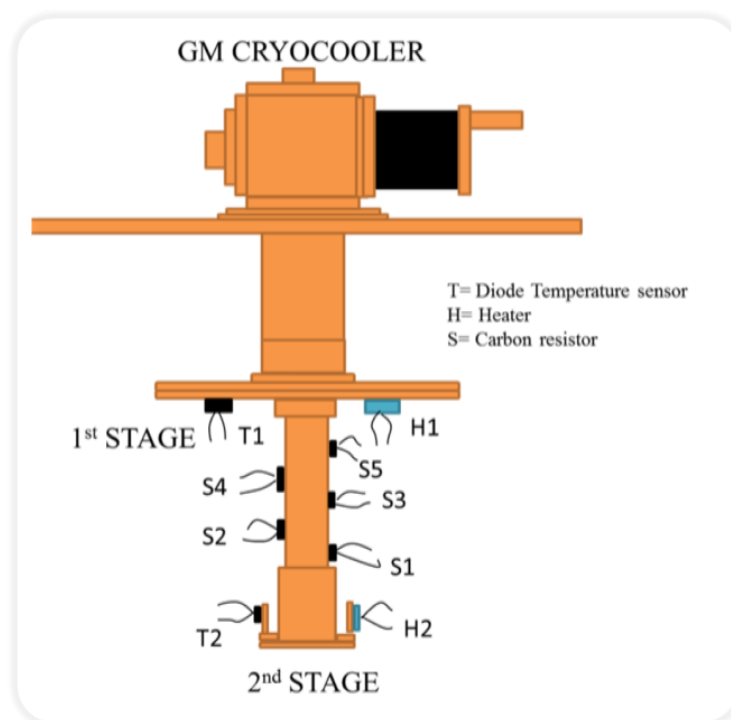


Fig .4.13: Schematic diagram of the test setup.

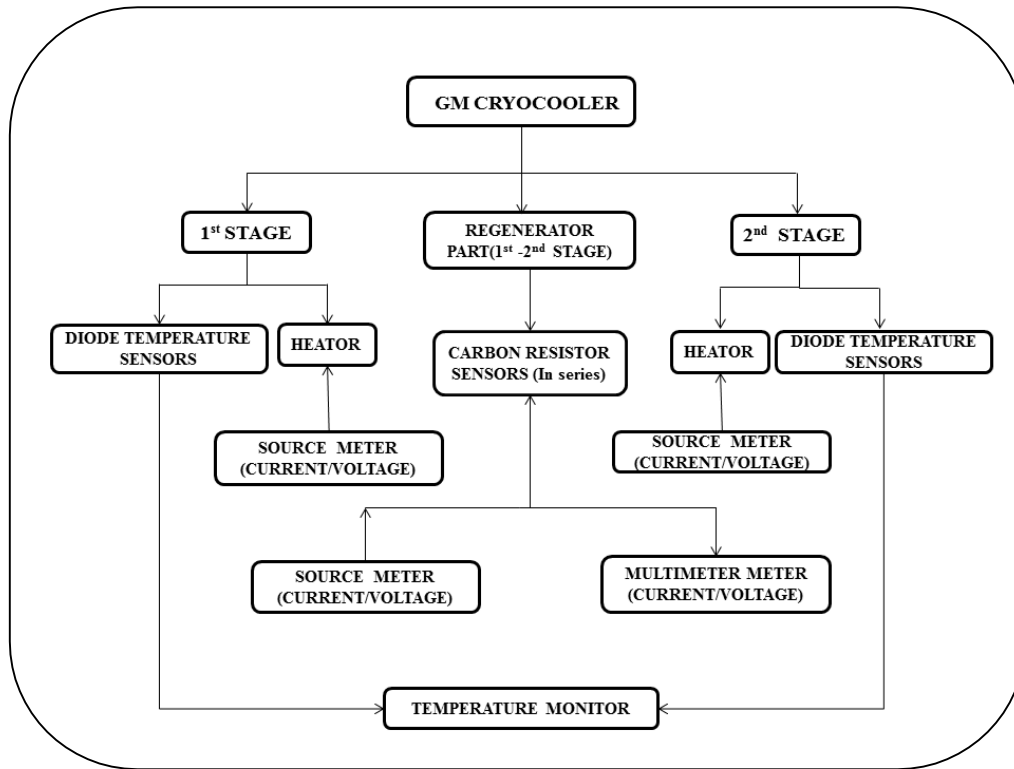


Fig.4.14: Block diagram for the test set up.

4.4.2 Experimental procedure for the generation of cooling curve

After the Integration of the whole system, a turbo molecular pump based pumping system has been attached to the cryostat to generate the vacuum. To measure the vacuum level, a Penning gauge (Pfeiffer Vacuum) has been attached to the cryostat. A dual gauge display (Pfeiffer Vacuum) has been used to monitor the vacuum. When the vacuum of the cryostat reached to $10\text{E-}04$ mbar level, the GM cryocooler has been started for cooling down the cryostat. The vacuum of the cryostat improved to $10\text{E-}08$ mbar due to the cryopumping by the cryocooler. At the steady state condition, the temperature of the 2nd stage of the cryocooler reached to 2.7K. The steady state temperatures of 1st stage cold head (T1) is 28.98K. These steady state temperatures correspond to the finite static heat load that is not zero. At this steady state, the voltage of each five carbon resistor S1, S2, S3, S4, S5 is measured individually by supplying current $100\mu\text{A}$. With the help of voltage, the resistance of each sensor can be calculated which directly will give the temperature at that position. The graph between Temperature and distance of sensors has been drawn which has been shown in fig.4.15. This curve has been generated under vacuum condition and with no external load applied manually.

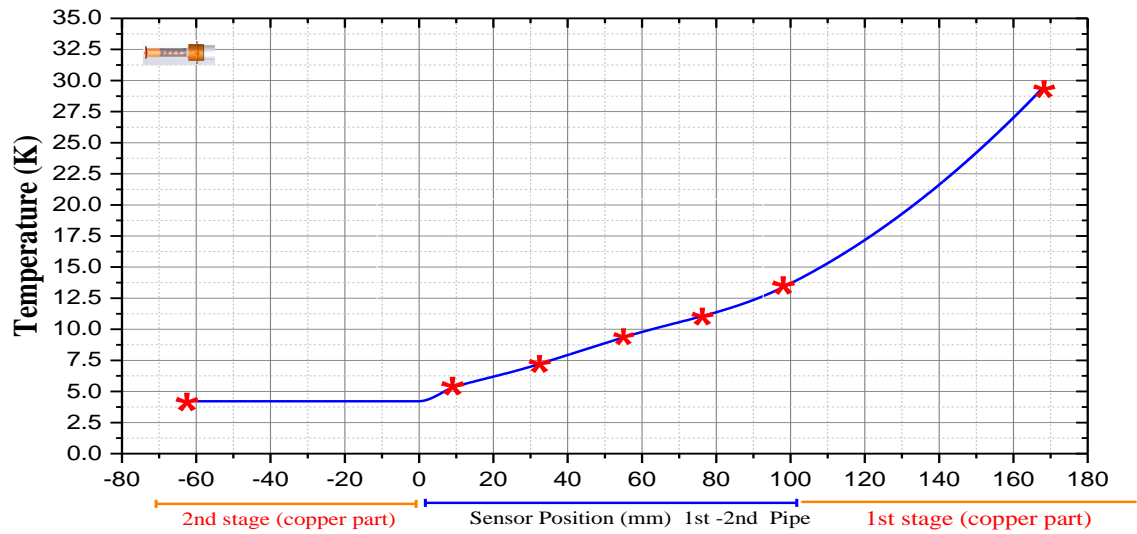


Fig.4.15: Cooling curve of two stage 1.5W at 4.2K (SRDK-415D) GM Cryocooler.

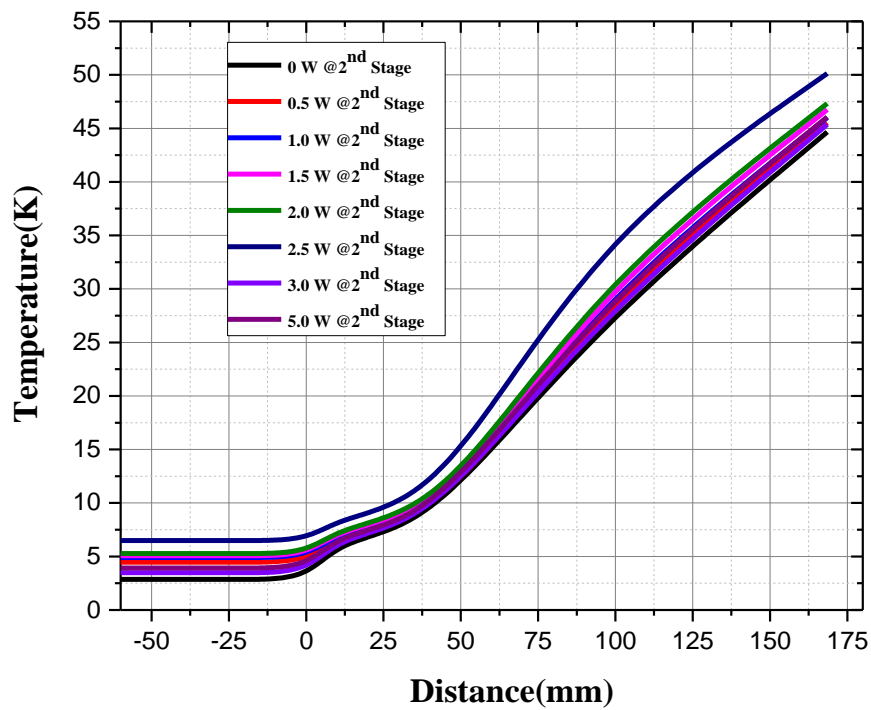


Fig.4.16: Cooling curve of two stage 1.5W at 4.2K (SRDK-415D) GM Cryocooler for 20W @ 1st Stage and varying load @ 2nd Stage.

Fig.4.16 represents the cooling curve at different heat loads. For this graph, Heat load at the 2nd stage of GM cryocooler has been varied from 0.5W to 5W but the heat load at 1st kept constant of 20W. This graph shows that as we increase the load on 2nd stage of GM cryocooler the cooling curve shifted towards the right that shows that 1st stage temperature also rise.

4.4.3 Cooling curve by considering different type of Heaters

Case 1:

Fig.25 shows that different position of sensors and wire heater for the generation of cooling curve. In this case, a heater in a rectangular shape having resistance value 50Ω has been used for powering the intermediate stage as shown in fig.4.17. The cooling curve generated by this method is shown in fig.4.18. This curve shows that as the power given to the heater, the curve rises to higher temperature sharply, but the 2nd stage temperature remains same and 1st stage temperature rises little higher value. This shows that the inter-stage cooling is available in the two-stage GM cryocooler.

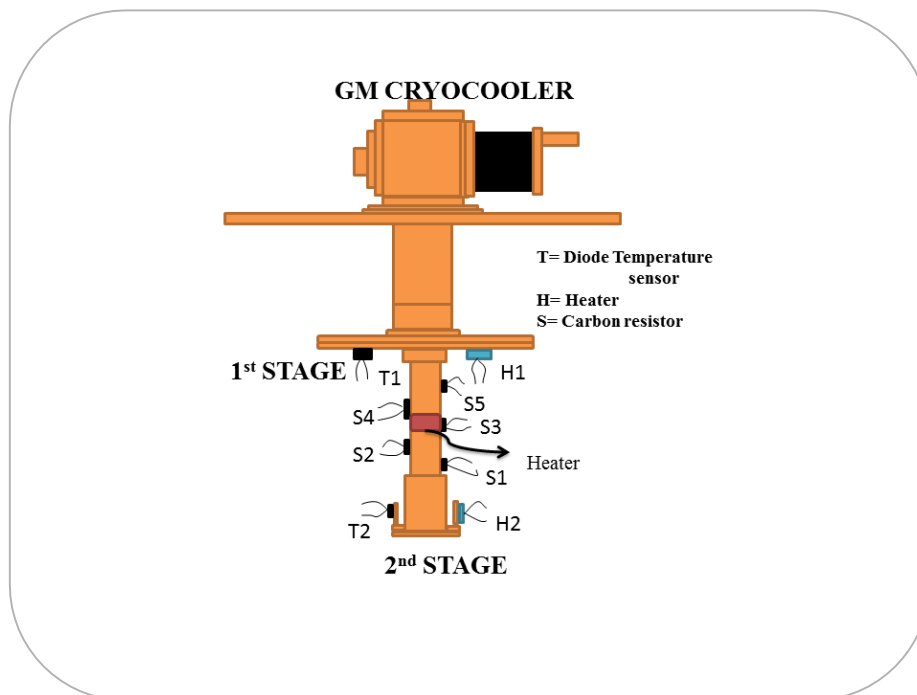


Fig.4.17: Schematic Diagram for test setup for the thin rectangular heater.

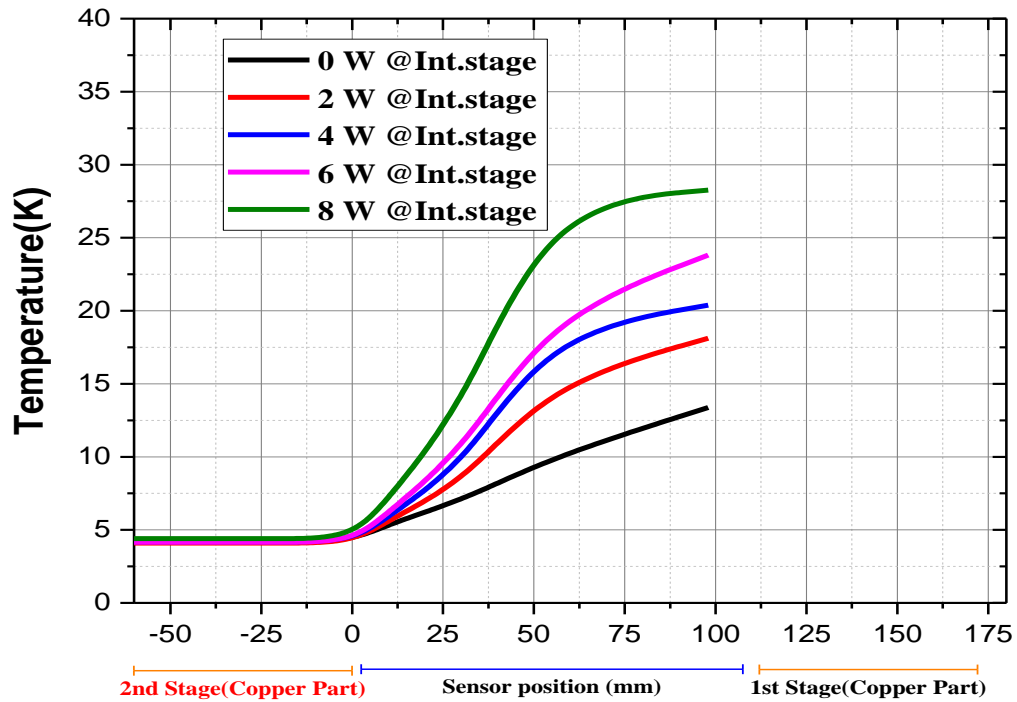


Fig.4.18: Cooling curve of two stage 1.5W at 4.2K (SRDK-415D) GM Cryocooler for heating at an intermediate stage with 50Ω Heater.

Case 2:

In this case, a wire heater having resistance value 9Ω has been used for powering the intermediate stage as shown in fig.4.19. The cooling curve generated by this method is shown in fig.4.20. This curve shows that as the power given to the heater, the curve rises to little higher temperature but the 2nd stage temperature remains almost same. The 1st stage temperature rises little higher value. This result also shows that in case of uniform heating the interstage cooling is available.

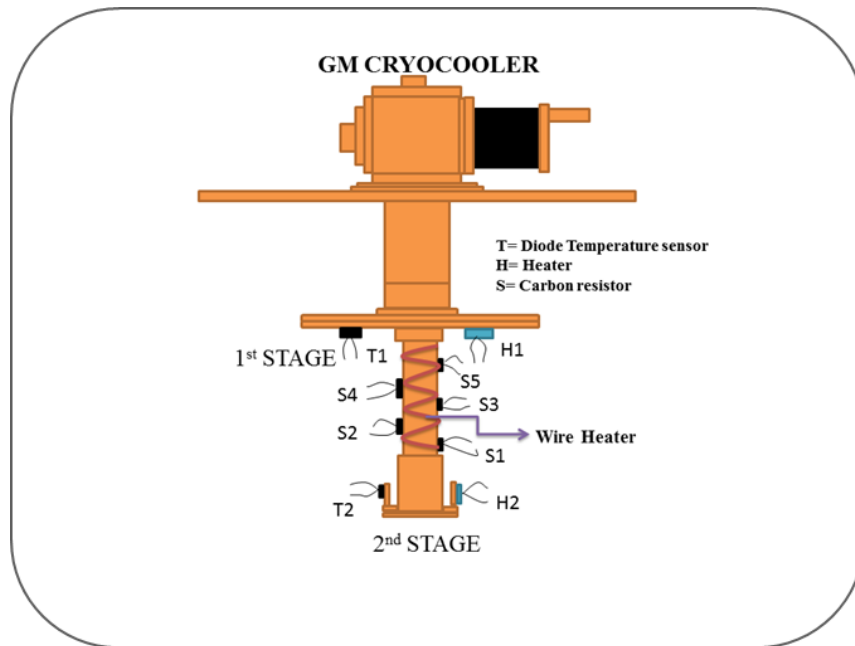


Fig.4.19- Schematic Diagram of test setup for wire heater.

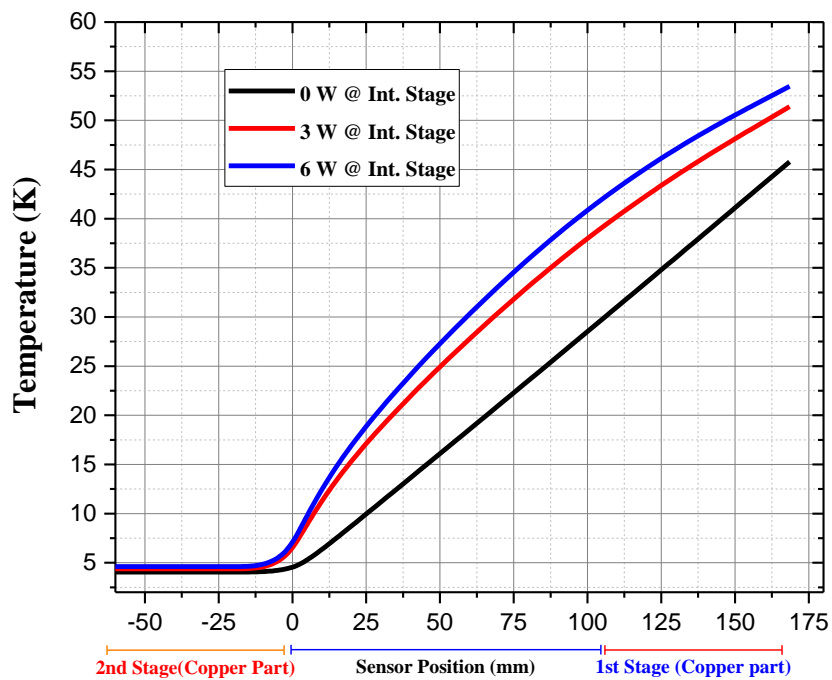


Fig.4.20: Cooling curve of two stage 1.5W at 4.2K (SRDK-415D) GM Cryocooler for heating at an intermediate stage with Wire Heater.

4.5 Mass flow controller and modular

We have used DFC digital mass flow controller and SDPROC Command Modules made by **AALBORG** to control the flow rate. The DFC digital mass flow controller is connected in the helium transfer line and is controlled by the command modular. This flow meter is calibrated with the helium flow. The DFC mass flow controller and Command module is shown in fig.4.21

Principle of operation of flow controller

The surge of helium gas entering the mass flow transducer and this gas is divided by diverting a little portion of gas to flow through a narrow stainless steel sensor tube. The rest of gas moves through the primary stream channel. The geometry of primary channel and stainless steel sensor tube are intended to guarantee laminar steam flow in every branch. According to principle of fluid dynamics, the flow rate of gas in the two laminar flow channel is proportional to the one other. Thus, the stream rate measured in the sensor tube is specifically relative to the aggregate flow through the transducer. So as to sense the stream in the sensor tube, the heat flux is introduced at two segments of the sensor tube using precision wound heater sensor coils. Heat is exchanged through the thin wall of sensor tube to the gas streaming inside. As gas flow takes place, heat is carried by the gas stream from upstream coil to downward stream coil windings. The resultant temperature dependent resistance differential is detected by the electronic control circuit. The measured gradient at the sensor winding is directly corresponding to the momentary rate of stream occurring. An output signal is generated that is a function of the amount of heat carried by the gases to demonstrate mass molecular based flow rates.



DFC digital mass flow controller



SDPROC Command Modules

Fig.4.21: DFC digital mass flow controller and SDPROC Command Modules.

4.6 Condenser

A long fins type condenser made with the help of **I-DESIGN Engineering Solutions Ltd.** has been used to provide additional surface area for condensation of helium at the 2nd stage of GM cryocooler. The surface area of long fin condenser is around 0.2 m². This Condenser has been bolted to the cold heads heat exchange with indium foil for good thermal contact and acts as an extension of it to provide an extra area for condensing gases. The long fins condenser has been shown in fig.4.22.

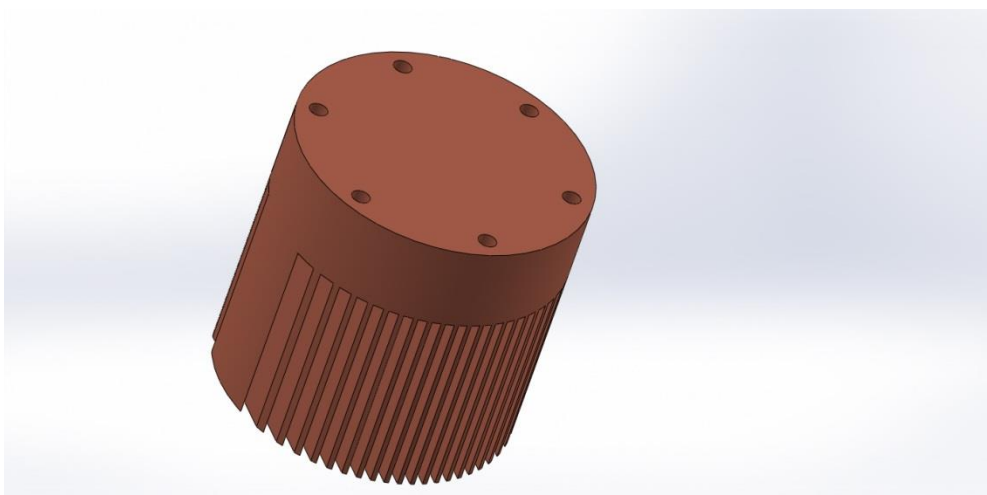


Fig.4.22: Condenser

CHAPTER 5
FABRICATION OF DEWAR
AND ASSEMBLY

FABRICATION OF DEWAR AND ASSEMBLY

5.1 Fabrication of Dewar

A Dewar which is known as cryogenic reservoir vessel use to store liquid helium or liquid nitrogen. A cryogenic dewar consists of storage vessel and which is surrounded by vacuum jacket that isolates the storage vessel from atmospheric conditions. This storage vessel is super insulated with MLI to reduce radiation heat load from atmospheric condition. The whole cryogenic dewar assembly has been made with the help of **I-DESIGN Engineering Solutions Ltd.** The whole assembly has been made with the help of 0.5mm SS304 thick sheet and 0.5mm thick copper sheet to reduce the mass. To make a 2 Ltr. reservoir capacity, assembly of wall thickness 0.5 mm is TIG welded with the end plates of thickness 0.5 mm. The whole assembly has been made with the help of TIG Welding and Brazing. The whole assembly has been leak tested with MSLD (Mass spectrometry Leak Detector) for any leaks. The Helium leak tightness was $<1.1 \times 10^{-9}$ mbar Ltd/sec at 5.3×10^{-2} mbar that is acceptable in case of dewar for the storage of helium. The whole assembly was subjected to cold shock test using liquid nitrogen at all the welds and joint. At low temperatures in SS304 some welding defects may present due to the thermal contraction and expansion at low temperature (77 K) to atmospheric conditions 300 K. Leak testing has been again done after pouring nitrogen.



Fig.5.1: Leak test of the cryogen reservoir assembly during cold shock with nitrogen and welding in flange of assembly.

5.2 Assembly of the dewar

All the welding joints where TIG welding and brazing has been done cleaned with alcohol and scrubber. All the o- rings has also been cleaned with alcohol and placed in respective O- ring grooves. The cryogenic reservoir vessel has been assembled with vacuum jacket and bolted to form vacuum seal with O-rings. This assembly has been tested for any leaks between cryogen reservoir and vacuum jacket with the help of MSLD leak detector.

Multi- layer insulation has been wrapped on the cryogenic reservoir vessel, neck part to reduce the heat load due to radiation. Up to 30 layers of MLI has been wrapped on the cryogenic reservoir to reduce the radiation load coming on the reservoir. If we wrap the MLI layers to tightly one above others than conduction and convection load between layers will increase because the air molecules would not get space to escape during pumping and high vacuum will not achieved. Approximately 30 layers of MLI have been wrapped on each other in 1cm of space.



Fig.5.2: MLI wrapping and assembling of the dewar

5.3 Assembly with GM cryocooler

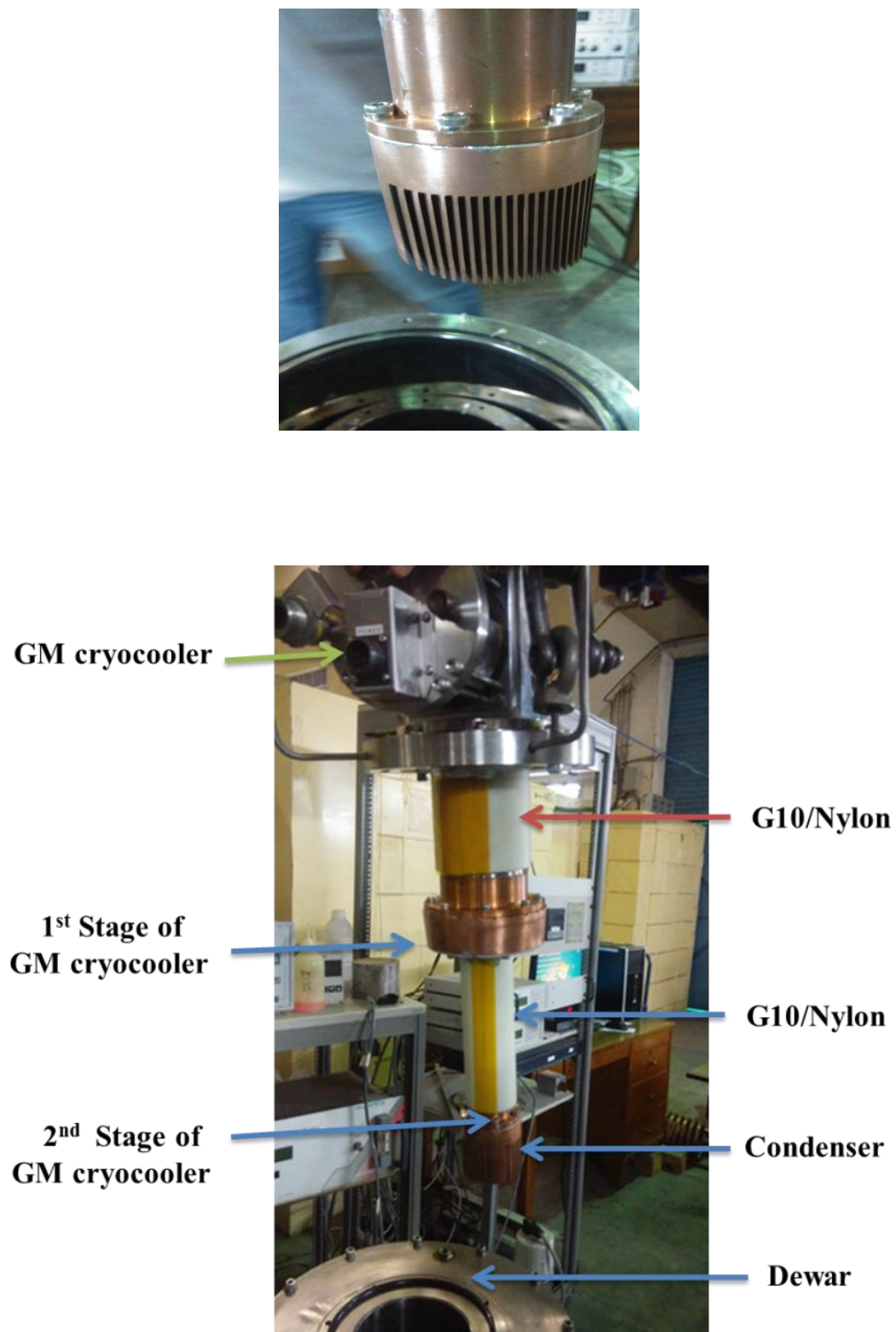


Fig.5.3: Final assembly of setup with GM Cryocooler.

CHAPTER 6

EXPERIMENTAL SETUP

AND RESULTS

CHAPTER 6

EXPERIMENTAL SETUP AND RESULTS

6. 1 Experimental setup for Helium liquefaction system

At first, assembly of the whole setup was done, and a Turbomolecular based pumping station has been connected to the dewar for vacuum. In dewar four diode sensors has been paced and one diode sensor placed on the 1st stage of cryocooler. The cold head of cryocooler with heat exchanger and other parts connected has been placed on top of the experimental dewar and bolted on the flange. O-ring has been used to seal the dewar and flange. The helium flex lines, motor cord, cooling water supply has been fitted to compressor package. We have also used stycast to seal properly the opening and the sensor wires. Gas was taken from the cylinder. The outlet from the cylinder was connected to valve controller and then it is connected to digital mass flow meter. Three ¼ inch pipe that has been welded for neck inlet, outlet and for sensor wires. The outlet port has been fitted with a 20 Psi relief valve, pressure transmitter (-1 bar - 1.5 bar).The pressure transmitter is connected at the outlet end so that the actual pressure of vessel can be observed during the liquefaction of helium at a particular pressure. The outlet of digital mass flow meter is connected to the neck inlet inlet to the vessel. All the sensor wires have been connected to temperature monitor and level reader respectively. To measure the vacuum level, a penning gauge (Pfeiffer Vacuum) has been attached with the cryostat. A dual gauge display (Pfeiffer Vacuum) has been used to monitor the vacuum.A rotary pump has also connected in transfer line for pumping and purging. After the Integration of the whole system was done, then a turbo molecular pump based pumping system has been attached to the cryostat to generate the vacuum. The actual experimental set is shown in fig.6.1.



Fig.6.1: Actual Experimental setup.

6.2 Operation

The entire setup was consistently purged with high- pressure helium gas for around 1 day to uproot any water vapour or anything before beginning the cryocooler, which can condensed on cold head therefore giving false reading. Helium gas has been supplied from the cylinder at 80 bar gauge pressure by utilizing an adaptable $\frac{1}{4}$ inch tube. We have also checked the leak in whole connections .joints with the help of soap solution after pressurizing the system at 10 psi. We have filled the cryostat with helium at a pressure of 2-3 psi than cryocooler has been started. Once the cryocooler starts, it takes around 7 hours to cool down to 7.6K temperature. The sensor shows the 7.6K temperature of a cryogenic vessel not 4.2K-5.2K due to improper thermal anchoring. Along with cooling down of hole setup during 7 hours the condensation of helium also started. The helium gas inside the dewar condense on the cold heads heat exchange part and trickles down to the cryogen store where it begins to cool the dewar. The production rate continues to increase until a steady state is reached after 7 hrs for a particular 2-3 psi pressure of the vessel. At steady state, the production rate reaches a maximum value. When the helium reservoir pot filled up after 7 hours then the flow rate decreases sharply, and the pressure of vessel increases.

6.3 Experimental Results

Temperature shown by the T7 sensor was 7.65K at the outer surface of the cryogenic reservoir. This higher temperature shown by sensor T7 is due to improper thermal anchoring of wires of the sensor. Some amount of radiation load also coming from copper shield that is at 53K because sensor was attached outside surface of cryogenic vessel

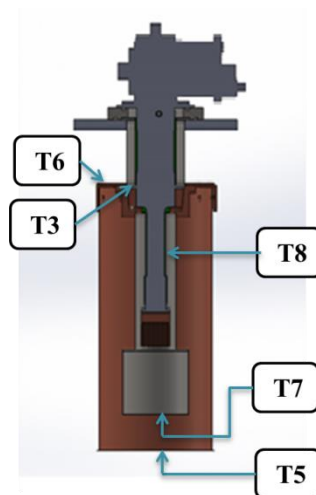


Fig.6.2: Position of temperature sensors.

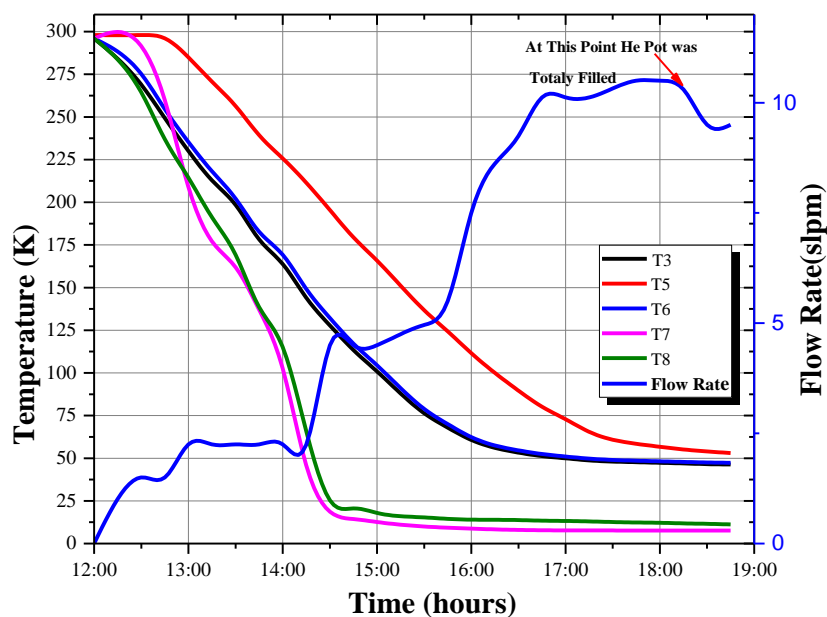


Fig.6.3: Cool down the curve and flow rate during liquefaction of Helium.

During the operation the vacuum of the vacuum chamber continuously increases, and the helium pressure in the cylinder decreases. The flow meter also shows the total amount of helium passed through the flow meter during operation.

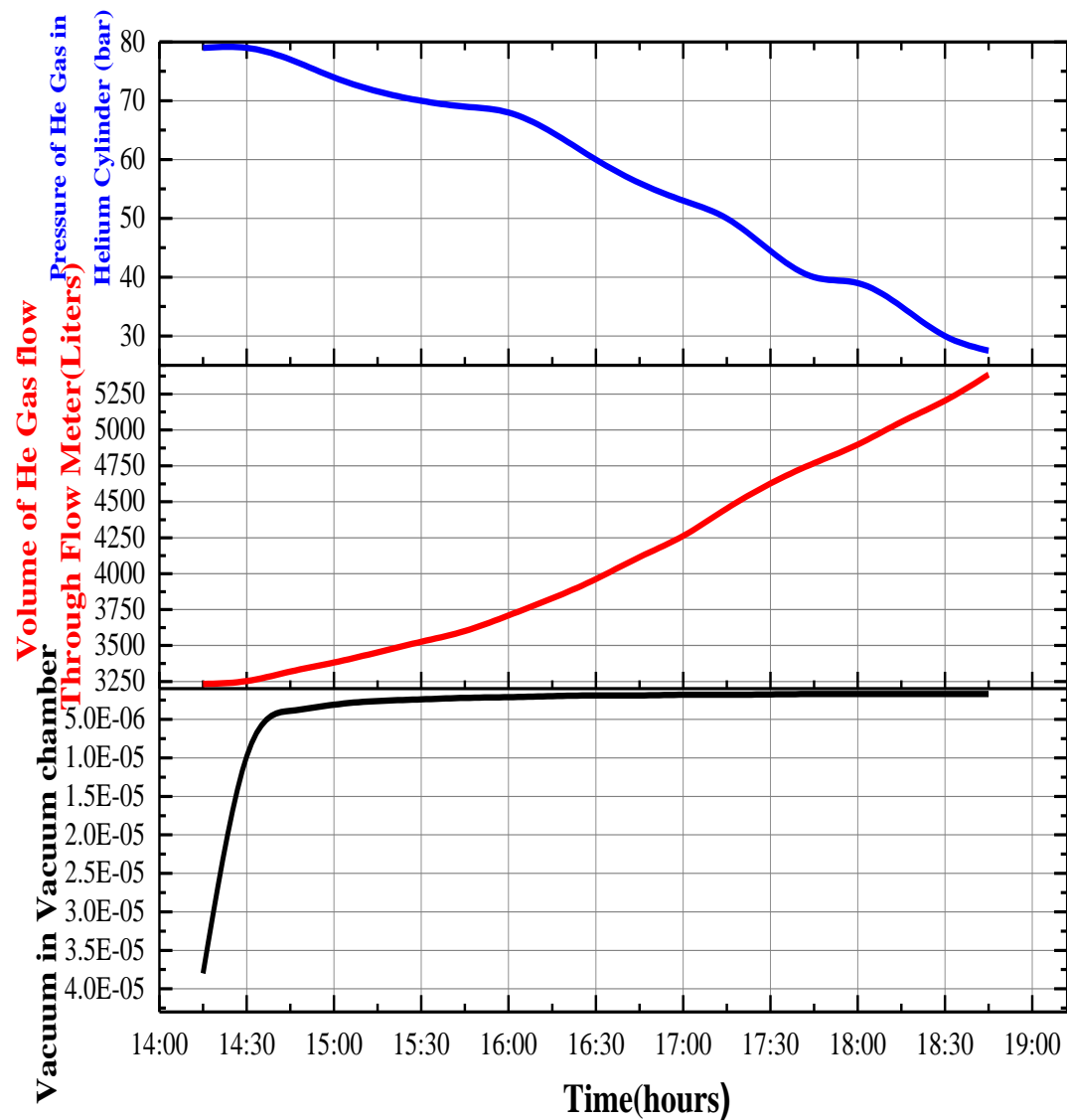


Fig.6.4: curve shows during operation vacuum increases, pressure of cylinder Decreases, total helium flow increases.

6.4 Calculation

$$Q = \dot{m}C_P\Delta T + \dot{m}L$$

Q = Heat Load (watt)

\dot{m} = Mass flow rate (kg/sec)

C_P = Specific heat of Helium gas at constant pressure (j/kgK)

ΔT = Temperature Difference (K)

L = Latent Heat (j/kg)

Table 4.2- Production rate at different outlet temperature at the 2nd stage of GM cryocooler

T ₁ (Initial Temp.)	T ₂ (final Temp.)	Mass flow rate(g/s)	Mass flow rate(lit./day)
300 K	4.2 K	9.633 X 10 ⁻⁰⁴	0.6658
20 K	4.2 K	1.4556 X 10 ⁻⁰²	10.06
17K	4.2K	1.736X10 ⁻⁰²	12
13.64K	4.2K	2.17X10 ⁻⁰²	15
10 K	4.2 K	2.9343 X 10 ⁻⁰²	20.26
5 K	4.2 K	5.9631 X 10 ⁻⁰²	41.21

From table 4.2 we can say that if we use the precooling effect of the GM cryocooler than the liquefaction rate will increase. We have achieved the liquefaction rate of 20 lit./day, which shows that near 2nd stage of cryocooler the helium gas temperature will be nearly about 10K.

CHAPTER 7
NITROGEN LIQUEFACTION
WITH GM CRYOCOOLER

CHAPTER 7

NITROGEN LIQUEFACTION WITH GM CRYOCOOLER

7.1 Principle used for Liquefaction of Nitrogen

For the production of liquid nitrogen, we have separated nitrogen from the air with the help of separation unit and purified by the purifier unit and then cooled up to 77 K for condensation. Along with the Condensation of liquid nitrogen, storage of liquid nitrogen is also important problem; Because nitrogen stays liquid at 77 K, by exposing to atmospheric conditions liquid nitrogen will not stay in liquid state for long time. Cryogenic storage tanks and Dewars have been designed and manufactured to store liquid nitrogen in it. These vessels are vacuum jacketed (double walled) to separate the vessel which carrying the liquid nitrogen from atmospheric conditions. The space between them is evacuated to reduce convection loads, and 35 layer of multi-layer insulation has been utilized to diminish radiation load coming from outer vacuum vessel at 300K to inner cryogenic reservoir at 77 K. In this project a commercially available single-stage Cryomech GM cryocooler has been used to provide cooling and condensation at 77K. The rated refrigeration capacity provided by the company for this cryocooler at 80 K is 266 W. The cold head mounted into the top of the dewar, and it reaches out down into the neck of the dewar with the end goal of cooling the nitrogen gas entering the dewar to 80K at diverse pressure of cryostat. The nitrogen gas condenses on contact with the cold head heat exchanger. The condensed nitrogen trickles off the heat exchanger down into the dewar. This procedure would ordinarily bring down the pressure inside the dewar, but the controller permits more nitrogen gas to enter the dewar to keep up the pressure at the preset level. The stream rate of the nitrogen gas into the dewar is controlled by the rate of liquefaction inside the dewar. So with the accessible refrigeration capacity of cold head we have fluctuate the working pressure of dewar from 3psi to 15 psi to obtained maximum production rate of of 82 Lit/day at 15 psi in 28 liter experimental dewar. We have liquefied nitrogen that is taken from two different sources. Firstly, nitrogen is separated from compressed air by membrane having oxygen percentage 4-5% has been liquefied. Secondly, nitrogen vapour(pure nitrogen) is taken from the liquid nitrogen cryostat that is at IUAC New Delhi. We have also compare the result obtained by two type of nitrogen source.

7.2 Principle Components of Nitrogen Liquefier

7.2.1 Gifford-McMahon cryocooler

A new thermodynamic cycle was introduced by W.E Gifford in the year 1959 that could be used to make cryogenic refrigerators. Gifford–McMahon (GM) cryocoolers were first developed in 1960 which was based closed cycles. In 1980s, Gifford-McMahon cryocoolers were used to cool charcoal absorber about 15 K in cryopumps. Their utilization in cryopump in semiconductor fabrication equipment for delivering clean vacuums gave a substantial market for these cryocoolers and prompted numerous upgrades in their reliability and the decrease of their cost. Up keep interims of one to two years are commonplace for these cryocoolers and are normally part of planned maintenance of the whole manufacture equipments. The use of regenerator in 1990 made with the rare earth materials which have high heat capacity in the range of 4-20 K permitted the GM cryocooler to accomplish temperature of 4.2K. The commercial availability of the GM cryocoolers, both one and two-stage systems, has driven them to utilized for many development projects involving new applications.

We have used single-stage Cryomech cryocooler with the refrigeration capacity of 266W at 80K and it goes up to 25K at NO Load condition. Their cost and effective cooling capacity at 80K is the reason to choose this cryocooler. The main objective of this project was to achieve the production rate more than 70 lit/day. So, a higher refrigeration capacity cryocooler was chosen. The cost of pulse tube cooler is higher than GM cooler and also consumes more power than GM cooler.

Component of Gifford-McMahon cryocooler

Regenerator /displacer – Displacer is used to move the gas from one end to other end and during this process gas exchange heat from regenerator. The gas is always expanded at cold end.

Compressor – Compressor is use to circulate the helium through cold head and the heat of compression is removed by continuous supply of water or air through the compressor.

The regenerator – It acts as a “cold store”. After the gas is expanded it passes through the regenerator and exchanges the “cold” with the regenerator material and passes back to the

warm end. On the other half of the cycle as the gas goes towards the cold end it is pre-cooled by the regenerator. It is made up of rare earth material.

The rotary valve –It is driven by motor to switches the cold head from high pressure side to low pressure side.

Flex Lines- Helium flex lines are stainless steel hose to transfer helium gas from compressor to the cold head and again back. It is a leak proof detachable line.

Specification of GM Cryocooler (courtesy of Cryomech Inc.)

Cold head: AL300

Weight.....	41 lb. (18.6 kg)
Cooling Capacity.....	266W @ 80K
Cool down time.....	15 minutes to 80K
Lowest temperature.....	25K with no load

Compressor Package: CP2800

Helium static pressure	15.9 ± .34 bar (230 ± 5 PSIG)
Weight.....	119 kg
Electrical Rating.....	200/230 or 440/480VAC, 3Ph, 60Hz // 200 or 380/415VAC, 3Ph, 50Hz
Power Consumption @ Steady State.....	5.5//6 kW

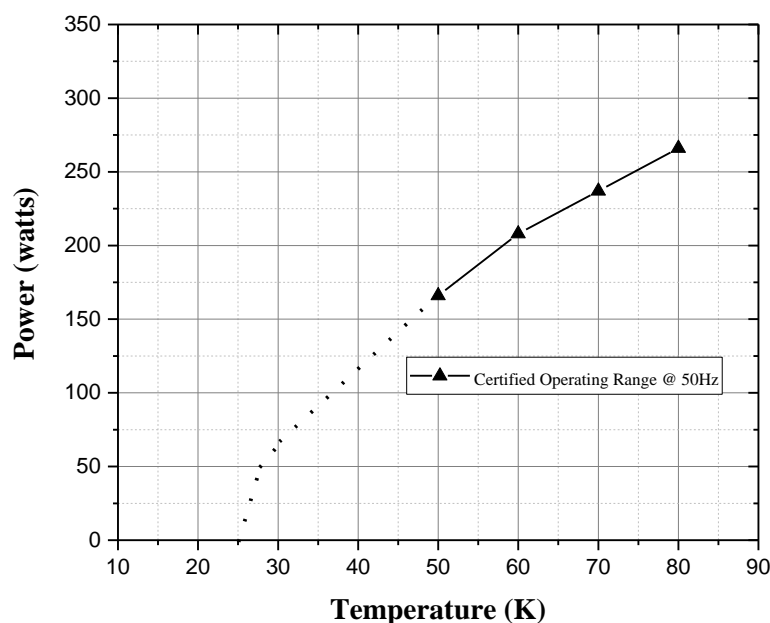


Fig.7.1: Cooling Capacity curve of AL300 GM cryocooler

7.2.2 Dewar for Liquid Nitrogen

Dewar for liquid nitrogen consists of a cryogen reservoir along with vacuum jacket which separate the reservoir from atmosphere. Dewar used in this setup has all welded construction. Dewar consists of evacuating valve for the generation of vacuum with the help of Turbomolecular pumping station. If vacuum is not order of 10^{-5} mbar or above, then due to large number of molecules, conduction through gas increases between vacuum jacket and cryogen reservoir. A 15 psi relief valve has been attached in this dewar for safety purpose. The cryogen reservoir in this dewar is made up of stainless steel. Vacuum of the order of 10^{-5} mbar is necessary between cryogen reservoir and vacuum jacket for liquid nitrogen. This order of vacuum is required to reduce the conduction load(in milliwatt range) at the cryogen reservoir at 80K. To reduce the conduction load, stainless steel neck or G10 has been used between them for support. This will reduce the conduction load between them. The other heat load is radiation heat load that overtake the convection load in vacuum condition. In case of liquid nitrogen reservoir, radiation load is almost 45w/m^2 which is very high. So, we have wrap multi-layer insulation on cryogen vessel to minimize the radiation load. MLI is highly reflective material. MLI is an insulation consisting of multiple layers of thin aluminium sheets with high reflectivity intended to reduce the radiation load on the cryogen reservoir. The thickness of aluminium is in the range of 5 to 10 nm on Mylar film. A fibrous material of low emissivity and thermal conductivity is placed between the layers, which acts as a thermal insulator between the layers.

7.2.3 Rotary and Turbomolecular Pumping Station

Rotary pump is used as backing pump for diffusion or Turbomolecular pump. This pump gives vacuum of 10^{-2} mbar for single stage and 10^{-3} mbar for double stage pump. This vacuum is not enough for liquid nitrogen dewar to operate between 77 K to 300 K. Turbomolecular pump is used for the production of clean high vacuum. This pump is based on principle that compression ratio is dependent on the mass of molecules. The heavier molecules like oil particles can be easily removed and no back streaming of oil particles occurs and we get a clean vacuum.

In the range of higher vacuum the number of molecules is very less thus the mean free path between them is larger so, the collision of molecules with each other is less frequent than

with the wall of rotating blades, hence increasing the influence of rotating blades on the molecules. This pump operates in the range of 10^{-2} mbar to 10^{-10} mbar pressure. We have used Turbomolecular based rotary pumping station to generate the required vacuum.

7.2.4 Level sensor

For the liquid nitrogen level measurement, we have used a capacitance based level sensors. This instrument has sensing element of $3/8^{\text{th}}$ outer diameter cylindrical type capacitor. This sensor allows the cryogenic liquid to become dielectric in the annular space. This instrument measures the sensor capacitance that is directly related to the percentage of the sensor immersed in the cryogenic liquid. The length of sensor is 1 m with the active length of 33 cm.

7.2.5 Vacuum Gauge

We have used Pfeiffer vacuum compact full range gauge (PKR 251) for the measurement of vacuum. This gauge is capable of measuring pressure from 1013 mbar to $5\text{E-}09$ mbar. This gauge consists of two measuring system that is Pirani and Cold cathode system; both are combined to give a single measurement system. The analog signal coming from this gauge is interpreted by Pfeiffer vacuum dual gauge to display the correct value of vacuum on digital display.

7.2.6 Mass Flow Meter

We have used a Aalborg GFM-47 mass flow meter for the measurement of nitrogen gas flow to the inlet. The working range of this device is 0-2 g/sec for liquid nitrogen and it can be used for other gas too, due to their dependency on the thermal conductivity and specific heat of that gas. The flow meter was calibrated with nitrogen gas for the particular range.

7.2.7 Temperature Monitor and Temperature Sensor

For displaying accurate temperature data from different types of temperature sensors, we have used temperature monitor to measure and interpret. A Lakeshore 218 temperature monitor is used to monitor the data coming from 8 silicon diode temperature sensors. This temperature monitor has eight channel input temperature sensor and which can be used as resistive or diode types of temperature sensors. Silicon diode sensor has been used as temperature sensor that is described in chapter 3. These sensors show good sensitivity in the range of 15K-300K. We have calibrated 8 number of Silicon diode sensors and used in the experiment.

7.2.8 Condenser

A long fins type condenser made with the help of **Vacuum Techniques Pvt.** has been used to provide additional surface area for condensation of nitrogen. The surface area of long fin condenser is around 0.2 m^2 . This Condenser has been bolted to the cold heads heat exchange with indium foil for good thermal contact and acts as an extension of it to provide extra area for condensing gases. The long fins condenser has been shown in fig.7.2

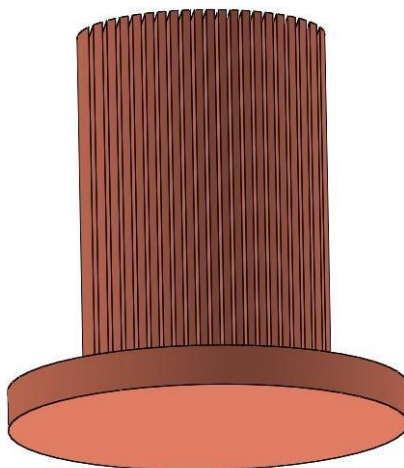


Fig.7.2: Condenser (HX2 with Long fins).

7.2.9 Filtration unit and Membrane Unit (N₂ Separator)

Compressed air contaminants come in three forms:-

- Particle
- Vapours
- Liquid Aerosols

There are different contaminants sources that contaminate the air into the system that are as follows:

- Built-In type

This occurs due to the poor manufacturing process. If machining of the part is not performed accurately then there is the formation of discontinuous chip and burr which led to poor surface finish and forms built in type contaminate.

- Rusting in steel parts
- Grit and oil inclusion due to bad seals.
- Wearing action due to moving parts.

Thus to remove all above contaminants from the compressed air we have use particulate filters, coalescing filters.

The membrane unit consists of Particulate filter, Coalescing Filter, Carbon adsorber and membrane nitrogen generator. All four are connected in series and used for basically filtration of air and removing oxygen, dust particles, water vapour, carbon particles, etc.

7.2.9.1 Particulate Filter

Particulate filter is called as after-filter. Generally, it is used after the desiccant air dryer to trap any fine desiccant particles present in line. It consists of fibrous materials which removes solid particulates such as dust, pollen, mould, and bacteria from the air. It has unique deflector plate that creates swirling of the air stream ensuring maximum water and dirt separation. It has excellent water removal efficiency. It has large filter element surface and provides low pressure drop.

7.2.9.2 Coalescing filter

Coalescing filter is made of coalesce. A coalescer is a technological device performing coalescence. It is primarily used to separate emulsions into their components via various processes; operating in reverse to an emulsifier. Approx. 78% of particulates in air are 2 microns or smaller. So, we need Coalescing filter.

There are two types of coalescers:

- **Mechanical coalescers:** It is used for filters or baffles to make droplets coalesce. A coalescer that operates by the method of physical alteration or involvement of a droplet is influenced by mechanical, or physical, means.
- **Electrostatic coalescers:** It uses DC or AC electric fields (or combinations). Electrostatic coalescers use electrical fields to induce droplet coalescence in water-in-crude-oil emulsions to increasing the droplet size.

.In coalescing filter smaller particles come together form larger droplets and when they pass through the elements fiber matrix eventually becoming large enough to be gravitationally removed. The coalescing filters should be installed after the pre-filtration unit so that particles of size 5 microns get separated in the pre-filtration unit.

7.2.9.3 Carbon Adsorber

Carbon adsorber uses activated carbon for filtration of compressed air. Due to its high degree of micro porosity, just one gram of activated carbon has a surface area in excess of 500 m², as determined by gas adsorption. Filters with activated carbon are usually used in compressed air and gas purification to remove oil vapours, odour, and other hydrocarbons from the air. The most common designs use a 1 stage or 2 stage filtration principle in which activated carbon is embedded inside the filter media.

7.2.9.4 Membrane Unit (for nitrogen generation)

The separation of nitrogen from air is basically done by two methods:

- **Adsorption Technology**

The adsorption gas separation process of nitrogen is based on the phenomenon of fixing various gas mixture components by a solid substance called an adsorbent. This phenomenon is brought about by the gas and adsorbent molecules' interaction. It allows production of high-purity nitrogen from air, whereas membrane systems are not able to provide up to 99.9995% nitrogen. This technology generates nitrogen at lower cost and creates less impact on the environment.

- **Membrane Technology**

Membrane technology operates on the principle of differential velocity due to which gas mixture component permeate the membrane. Difference in partial pressure on different membrane side considered as the driving force for gas separation. Gas is supplied with high pressure in to the membrane unit. Because of difference in partial pressure on external and internal membrane surface, the gas flow separation takes place.

We have used membrane technology that works on sieving mechanism to separate nitrogen. The complete setup of separation unit and filtration unit is shown in fig.7.3. The specification of membrane that is provided by **Parker Hannifin Corporation** are:

Model NO.- HiFluxx®DT604

- Nominal Condition-

Temperature: 20°C/68°F

Ambient pressure: 1013 mbar

Maximum Pressure drop: <0.3 bar

- Compressed Air Condition-

Maximum operating pressure: 13 bar(g)/188 psi(g)

Compressed Air Temperature Range: 2-50°C/ 36-122°F

Residual oil content: <0.01mg/m³

Particles: filtered at 0.01μ cut off

Relative Humidity: < 100% (non condensing)

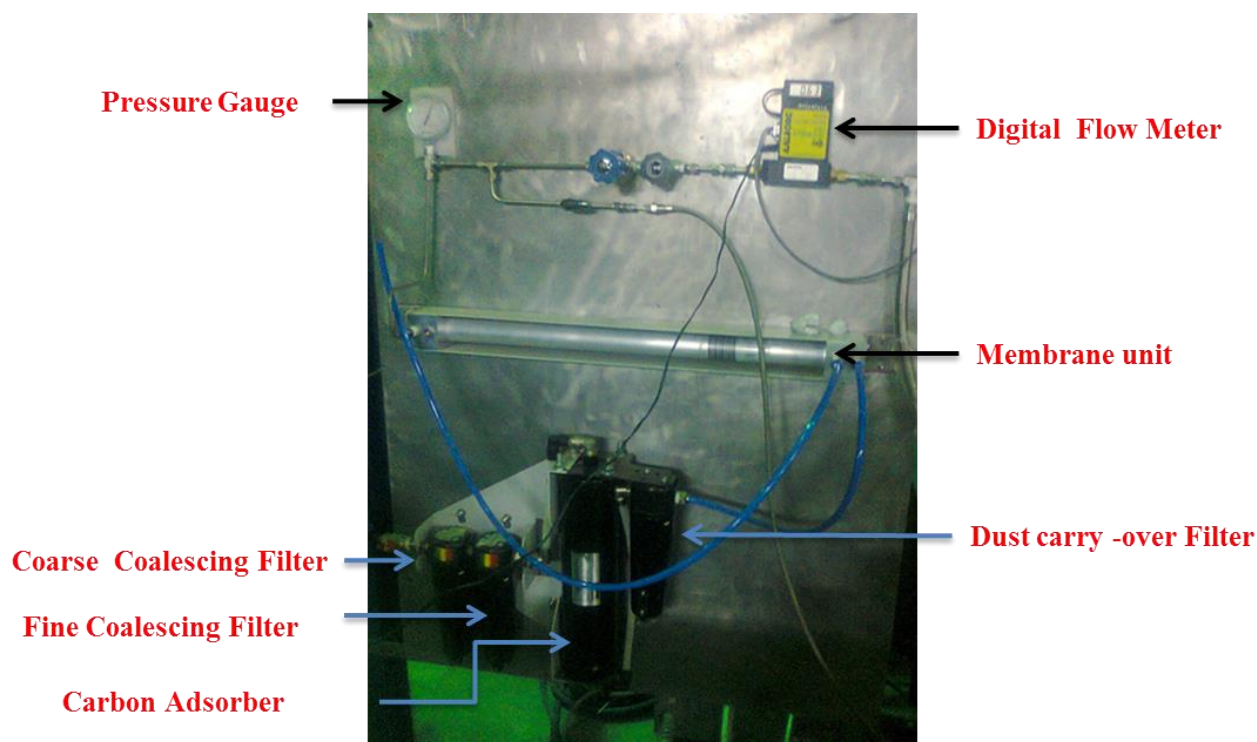


Fig.7.3: Actual complete setup of separation unit and Filtration unit.

7.2.9.5 Working of Separation unit and Filtration unit

Atmospheric air contains essentially 78% nitrogen and 21% oxygen. At first compressed air enters the coarse coalescing filter where a coarse particle of size 5 microns gets filtered. After coarse coalescing filter air enters to fine coalescing filter in which particle size of 2 microns or lesser than 2 microns gets filtered. Carbon absorber is attached after the fine coalescing filter unit to adsorb carbon, hydrocarbons, oil, moisture, etc. The dry compressed air is passed and filtered through the bundle of hollow membrane where nitrogen is separated from compressed air. Water vapor and oxygen goes safely to the atmosphere, but nitrogen gas is sent under pressure into bundle of membrane system. Pressure, flow rate and membrane size/quantity are the main variables that affect nitrogen production. Nitrogen purity (oxygen content) is controlled by throttling the outlet from the membrane bundle(s). At a given pressure and membrane size, increasing the nitrogen flow allows more oxygen to remain in the gas stream, lowering nitrogen purity. Conversely, decreasing nitrogen flow increases purity. By combining multiple membrane bundles, an infinite number of flow/purity ranges are available to satisfy practically any application that requires nitrogen gas.

CHAPTER 8
EXPERIMENTAL RESULTS
AND ITS ANALYSIS

CHAPTER 8

EXPERIMENTAL RESULTS AND ITS ANALYSIS

8.1 Experimental Setup for Nitrogen Liquefaction

At first, four diode sensors has been paced on the cryocooler surface and heat exchanger (HX2). The cold head of cryocooler with heat exchanger and other parts connected has been placed on top of the experimental dewar and bolted on the flange. O-ring has been used to seal the dewar and flange. The helium flex lines, motor cord, cooling water supply has been fitted to compressor package. The nitrogen separation unit (buffer) has been installed which is shown in fig.12. The outlet from separation unit is connected to the pressure gauge, and the outlet of the pressure gauge is connected to digital mass flow mete. In the ¼ inch pipe which was welded with flange for neck inlet, a Parker made 15 Psi relief valve, pressure transmitter(-1 bar - 1.5 bar) has been attached.The pressure transmitter is connected at the outlet end so that the actual pressure of vessel can be observed during the liquefaction of nitrogen at a particular pressure. The outlet of digital mass flow meter is connected to the side inlet to the vessel. All the sensor wires, Nitrogen level meter wires have been connected to temperature monitor and level reader respectively. To measure the vacuum level, a Penning gauge (Pfeiffer Vacuum) has been attached with the cryostat. A dual gauge display (Pfeiffer Vacuum) has been used to monitor the vacuum. An Oxygen percentage indicator has also been installed with the separation unit that shows the oxygen percentage in separated nitrogen from the air. After the Integration of the whole system was done, then a turbo molecular pump based pumping system has been attached to the cryostat to generate the vacuum. The entire experimental set has been shown in fig.8.1, and the actual experimental set is shown in fig.8.2.

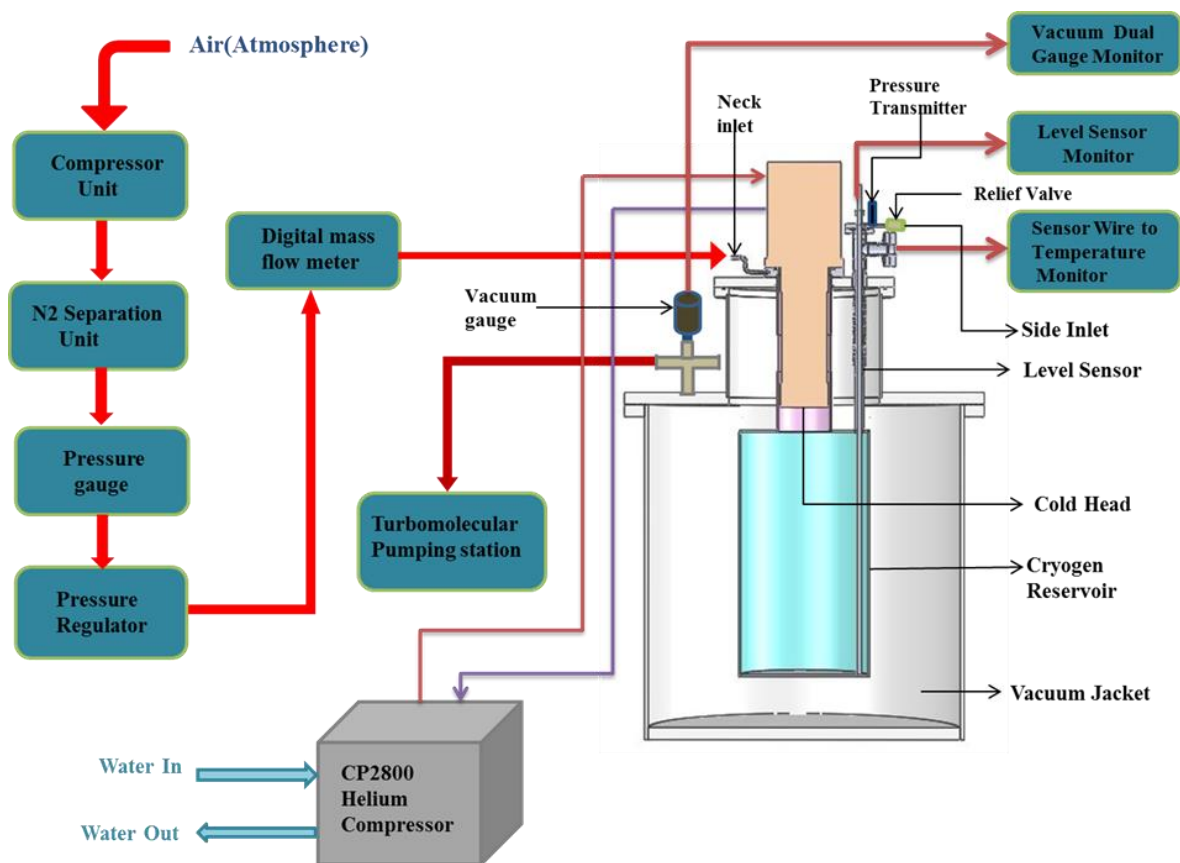


Fig.8.1: whole Experimental set up for Nitrogen liquefaction.



Fig.8.2: whole actual experimental set up for Nitrogen liquefaction.

8.2 Operation

Before starting of cryocooler the cryostat including all transfer line has been continuously purged with high pressure nitrogen gas. This helps in removing of water vapour present in cryostat which may condensed during operation of cryocooler. The operation of setup was done for different pressure and for different geometry to maximize the liquid nitrogen production.

After the starting of cryocooler, the cryocooler takes 15 minutes to reach the 80 K temperatures. Then nitrogen gas starts condensing inside the dewar and cool down the dewar. The production rate continues to increase until a steady state is reached after 3-4 hrs for a particular pressure of the vessel. At steady state, the production rate reaches a maximum value. The pressure is varied from 3psi to 15 psi to increase the liquefaction rate for geometry. For Each geometry (neck inlet, side inlet), the experimental run was done for 15-16 hrs. and the data was gathered for analysis. We have taken nitrogen from two different sources. For each nitrogen source, we have performed the experiment and comparison has been made.

8.3 Experimental Results

Experimental Run 1

In this experimental run, the inlet of nitrogen is through neck port. Fig.8.3 shows the temperature at the different position of cryocooler as well as the different position at cryogenic reservoir vessel when the liquefaction is done at 3psi with HX(Condensor). The curve for cooldown temperature of the cryocooler and the vessel with respect to time has been shown in fig.8.4. In this type of experimental run, pressure has been varied from 3 psi to 15 psi that is shown in tabular form in Table.1.

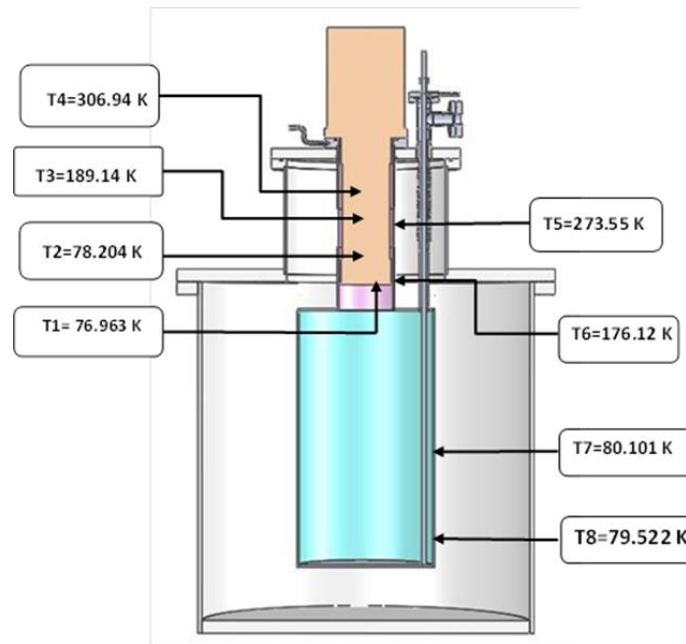


Fig.8.3: Temperature at different position of cryocooler and cryogenic reservoir vessel during liquefaction of nitrogen at 3 psi for inlet through neck port with HX2.

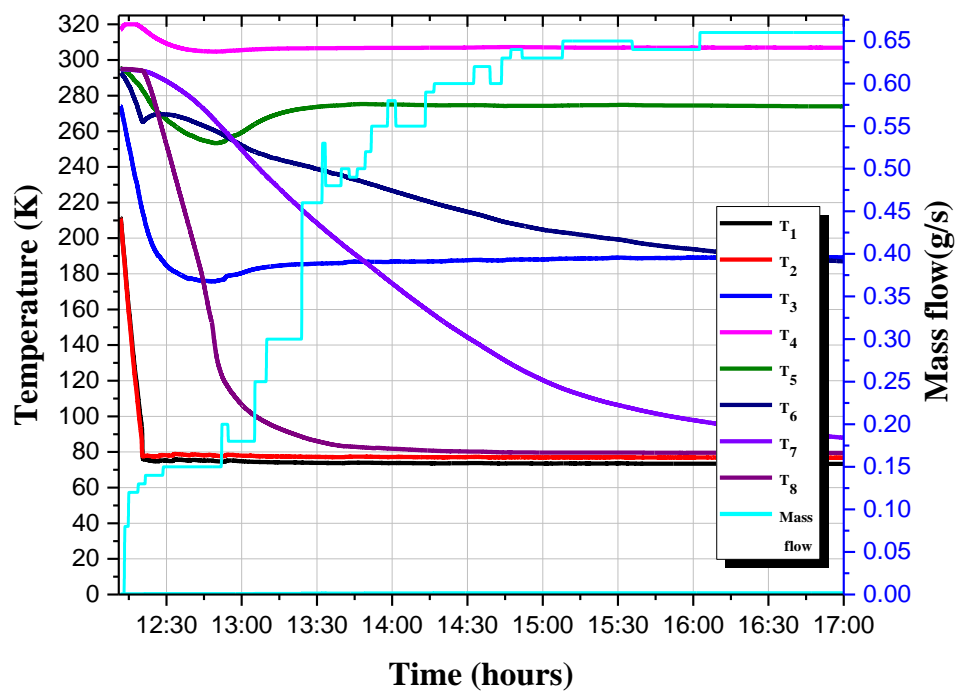


Fig.8.4: Cool down the curve for neck inlet at operating pressure of 3 psi.

Table 8.1- Observation table for Run 1

Entry N2 Gas	Neck Port
Operating Pressure	3 psi (0.206 bar) at steady state
Production Rate	74.36 Ltr/day at steady state
Condenser	Type II (HX2) (Long Fins)
Observations	<ul style="list-style-type: none"> ❖ Maximum production rate of 74.36 lit/day has been achieved at steady state , that can be seen from the sensors graph from T1 to T8 about 5 hrs after starting the cryocooler . ❖ Some amount of enthalpy has been taken by regenerator par from N2 gas because the temperature varies from 290K to 80K at heat exchanger part of the cold head. ❖ There is no theoretical formulation to predict the enthalpy removed, but CFD simulations can predict it.

Experimental Run 2

In this experimental run, the inlet of nitrogen is through neck port but condenser (HX2 with long fins) is not present. Fig.8.5 shows the temperature at the different position of cryocooler as well as the different position at cryogenic reservoir vessel when the liquefaction is done at 3psi.

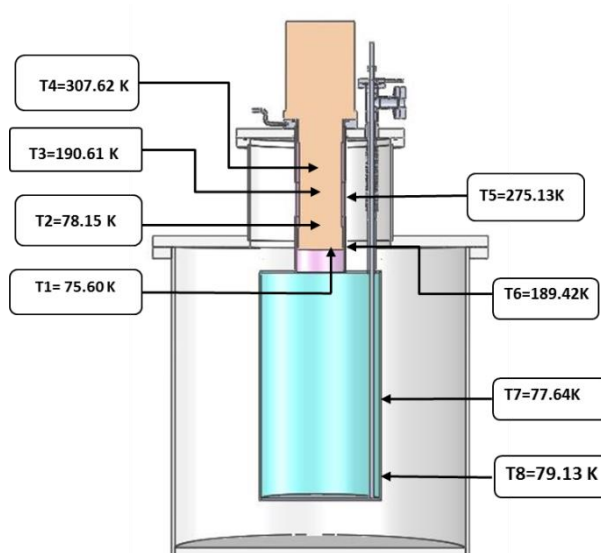


Fig.8.5: Temperature at different position of cryocooler and cryogenic reservoir vessel during liquefaction of nitrogen at 3 psi for inlet through neck port without HX2.

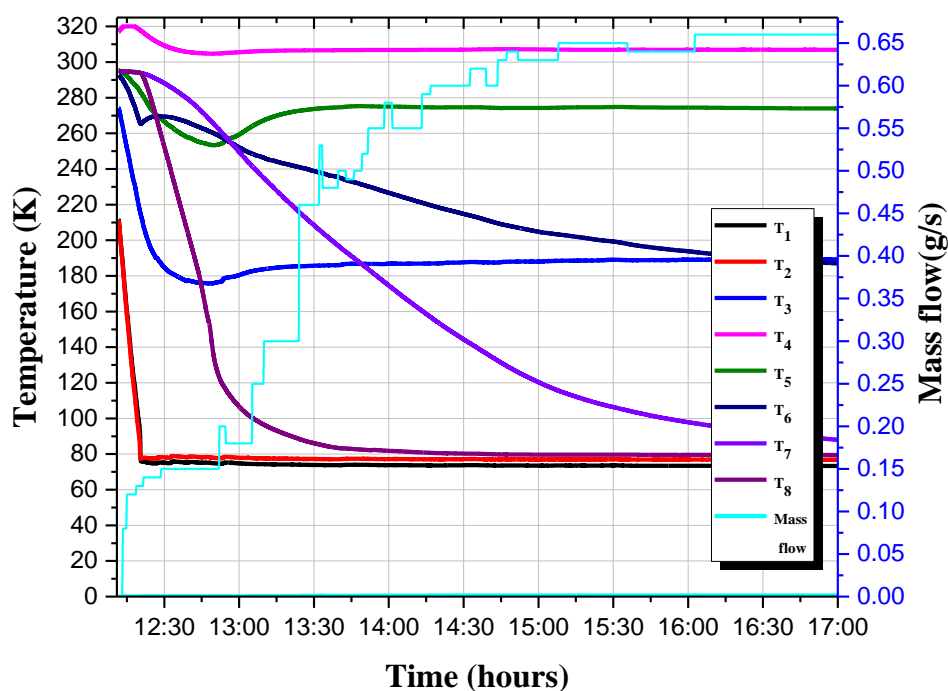


Fig.8.6: Cooldown curve for neck inlet at operating pressure of 3 psi without condenser.

Table 8.2: Observation table for Run 1

Entry N2 Gas	Neck Port
Operating Pressure	3 psi (0.206 bar at steady state)
Production Rate	71.08 Ltr/day at steady state
Condenser	NA
Observations	<ul style="list-style-type: none"> ❖ Nitrogen gas is flow through the cold head face and the neck of dewar thus temperature profile of cryocooler surface has been changed. ❖ From data we can predict that T1 is lower than T2 & T3 that means bottom part is used for cooling nitrogen gas. ❖ The maximum production rate of 71.08 Ltr/day was achieved at steady state condition that can be seen from sensors T1 to T8 around 5 hr after starting the cryocooler. ❖ Some amount of enthalpy has been taken by regenerator par from N2 gas because the temperature varies from 290K to 80K at heat exchanger part of the cold head.

We have varied the pressure from 3 psi to 15 psi for each inlet type of geometry. Pressure has been varied in the step of 3,6,9,12,15 psi. During the liquefaction period, each particular pressure has been maintained for at least 1 hour after the stable period have reached. The mass flow rate variation at different pressure has been shown in the graph given in fig.8.7. The graph has been shown for side inlet as well as neck inlet and for with or without condensor. From the figure, we can say that there is some amount of precooling is available in the AL300 GM Cryocooler because through neck inlet the liquefaction rate is higher. As we increase the pressure of vessel, the liquefaction rate also increases but at higher pressure further increment in liquefaction rate slows down. The graph shown in fig.8.7 is drawn when the nitrogen is separated from the air. The oxygen percentage, in this case, varies from 4-5%.

We have also taken pure nitrogen and nitrogen with impurity 4-5% for liquefaction and compared the results. Fig.8.8 show the variation of mass flow rate of nitrogen with respect to the pressure of vessel, when the vapour nitrogen at 300K is taken from liquid nitrogen dewar. This graph shown for the input of nitrogen gas through neck side of dewar only not inlet through side port. This graph shows that at lower pressure the liquefaction rate is lower in case of pure nitrogen comparison to impure nitrogen (4-5% of O_2). At higher pressure, both type (impure & pure nitrogen) of nitrogen gives the same amount of liquefaction rate.

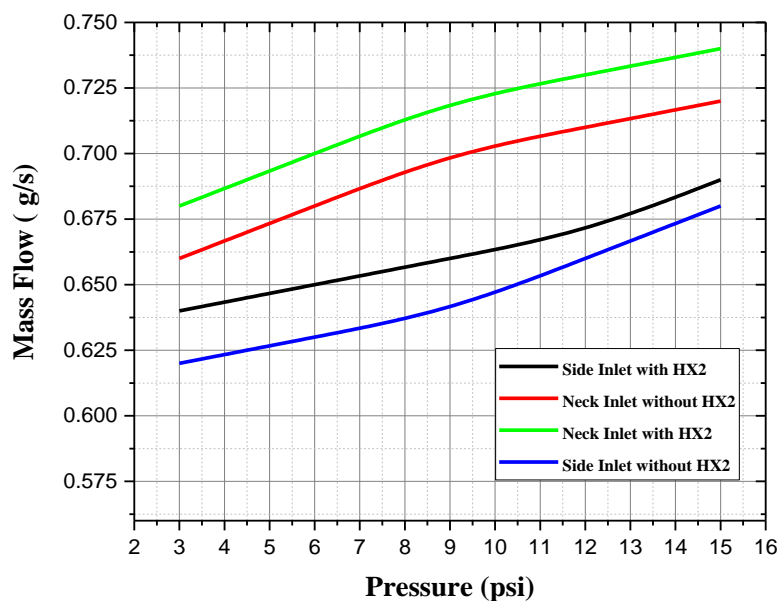


Fig.8.7: Graph of mass flow at a different pressure of vessel when nitrogen is taken from atmosphere.

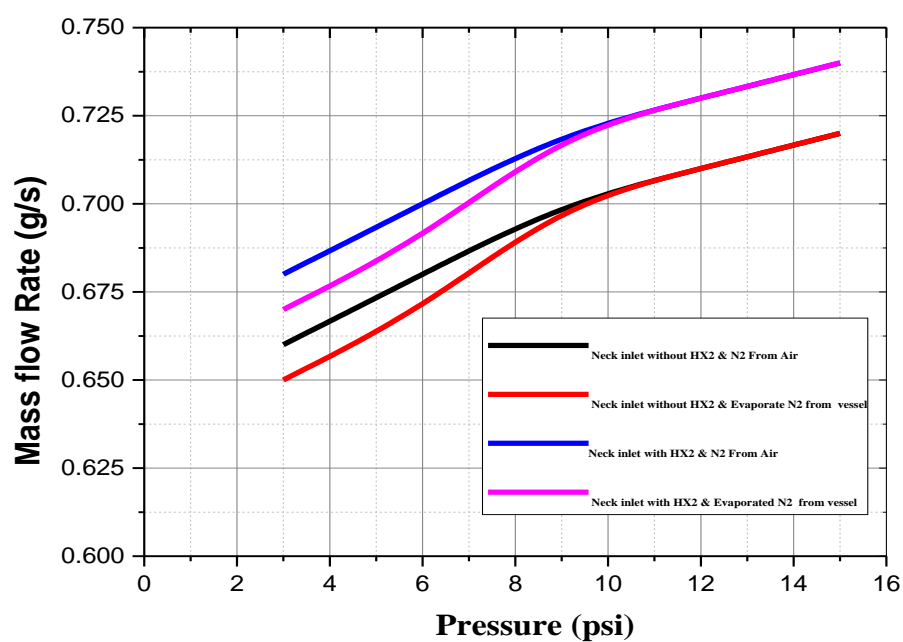


Fig.8.8: Graph of mass flow at different pressure of vessel when nitrogen is taken from atmosphere and vapour nitrogen from nitrogen dewar.

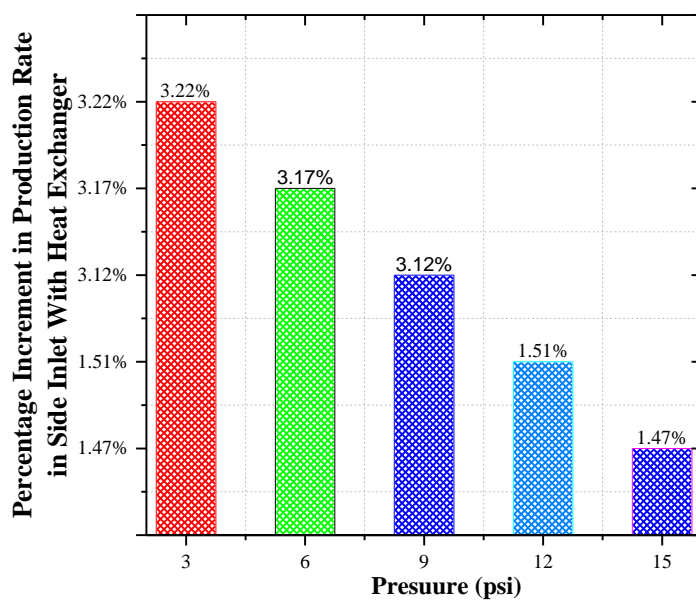


Fig.8.9: Bar graph of percentage increment in the production rate in case of side inlet with heat exchanger from base value (side inlet without heat exchanger).

Fig.8.9, fig.8.10 and fig.8.11 represent the percentage increment in production rate at different pressure from the base value (side inlet without heat exchanger). With the help of this pie chart, we conclude that due to the presence of condenser, the production rate increases. Production rate also increases when the inlet is through neck side due to precooling effect by the regenerative part of GM cryocooler. Thus, this three charts help in estimating the precooling power available at regenerator part and the efficiency of the condenser.

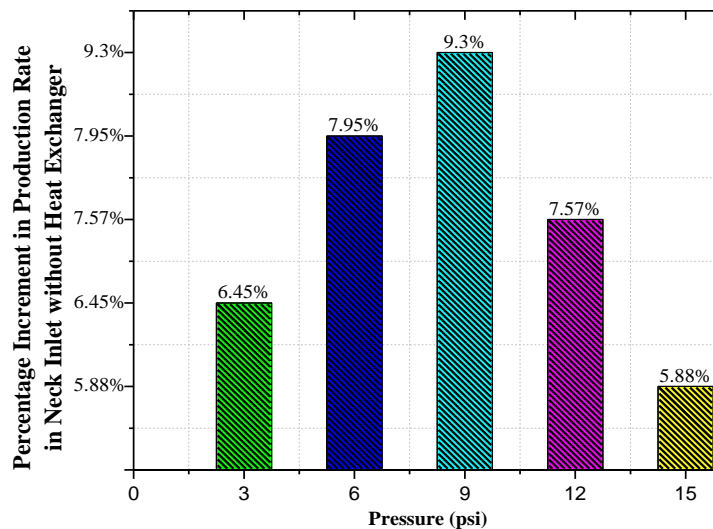


Fig.8.10: Bar graph of percentage increment in production rate in case of neck inlet without heat exchanger from base value (side inlet without heat exchanger).

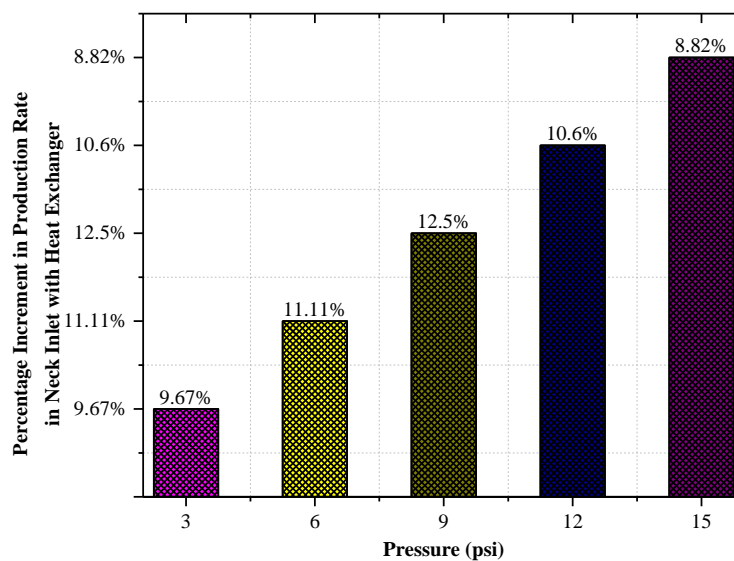


Fig.8.11: Bar graph of percentage increment in the production rate in case of neck inlet with heat exchanger from base value (side inlet without heat exchanger).

Fig.8.13 shows the cryocooler temperature at a different position for side inlet of nitrogen gas and also for neck inlet of nitrogen gas. This curve shows that during neck inlet the temperature of the cryocooler is increases in comparison to the side inlet of nitrogen. This rise in temperature through neck side inlet has been minimised by the precooling effect of cryocooler till the gas has been reached at the bottom (near condenser) for condensed. This curve also shows that the precooling effect is present in GM Cryocooler. This precooling effect can be used to increase the liquefaction rate. This curve shows that as the load increases on the cryocooler the curve shifted toward higher temperature side. Fig.8.12 shows the sensors mounted on different position of the GM Cryocooler.



Fig.8.12: Sensors mounted on the different position of the GM Cryocooler.

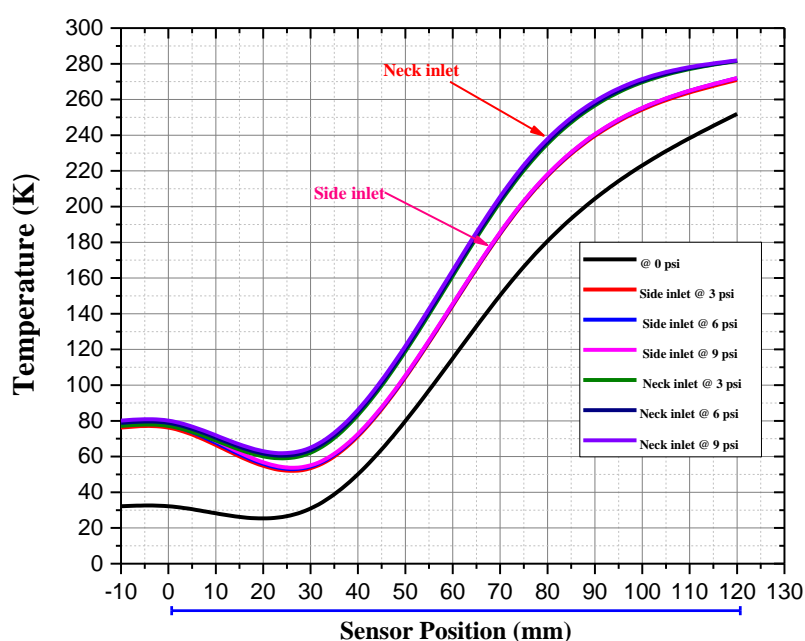


Fig.8.13: Cryocooler temperature Profile at various positions for side inlet of nitrogen gas and for neck inlet of nitrogen gas.

Summarised data of the experimental Run of Nitrogen Liquefaction

The summarised data of Nitrogen liquefaction is shown in Table 3 . This data is generated during nitrogen liquefaction when the air is taken from atmosphere and nitrogen is separated by using buffer unit .

Table No.8.3 :Summerized data of Nitrogen Liquefaction

Operation	N2 Inlet	T1 (K)	T2 (K)	T3 (K)	T4 (K)	T5 (K)	T6 (K)	T7 (K)	T8 (K)	Pressure (Psi) (gauge)	Vacuum (mbar)	Production Rate (Lit/day)
1	Neck Side Inlet (WITH HX2)	76.96	78.20	189.14	306.94	273.55	176.12	80.10	79.55	3	3.9E-5	74.36
		78.36	79.58	191.02	307.37	273.70	173.05	80.15	79.79	6	3.8E-5	76.55
		79.59	80.45	192.66	307.68	273.57	171.59	80.24	80.30	9	3.8E-5	78.74
		80.78	81.75	194.15	307.99	273.36	169.63	81.02	80.73	12	3.8E-5	79.83
		81.98	82.95	195.40	308.06	272.54	166.18	80.20	78.56	15	3.7E-5	80.93
2	Neck Side Inlet (NO HX2)	75.60	78.15	190.61	307.62	275.13	189.42	77.64	79.13	3	3.8E-5	72.18
		76.88	79.48	192.41	307.65	274.30	181.81	78.47	79.42	6	3.7E-5	74.36
		78.02	80.62	193.91	307.93	273.35	179.02	78.67	79.71	9	3.7E-5	76.55
		79.28	81.81	195.42	308.15	273.56	176.64	81.35	81.28	12	3.6E-5	77.65
		80.16	82.75	196.70	308.50	272.78	168.19	81.43	82.02	15	3.6E-5	78.74
3	Side Inlet (WITH HX2)	76.64	77.06	159.29	300.68	192.39	140.24	81.50	79.26	3	3.9E-5	69.99
		77.95	78.38	160.06	300.87	190.80	137.68	78.83	79.84	6	3.9E-5	71.08
		79.27	79.70	160.75	301.00	189.72	135.27	78.92	80.08	9	3.9E-5	72.18
		80.43	80.82	161.18	301.08	188.60	131.08	79.06	80.22	12	3.9E-5	73.27
		81.39	81.66	162.27	301.13	187.48	122.10	79.12	80.42	15	3.9E-5	75.46
4	Side Inlet (NO HX2)	75.81	77.61	165.85	302.23	220.01	207.47	117.4	79.60	3	4.2E-5	67.80
		76.82	78.55	165.30	302.68	211.23	187.96	79.07	80.71	6	4.2E-5	68.90
		77.78	79.59	163.46	302.58	200.25	161.57	79.42	81.14	9	4.2E-5	69.99
		78.66	80.57	161.76	302.53	192.79	138.03	79.59	81.38	12	4.2E-5	72.18
		80.58	82.31	169.29	303.87	212.43	198.47	82.43	79.62	15	4.2E-5	74.36

8.4 CFD Modeling for Nitrogen Precooling

We have numerically modelled the Nitrogen precooling up to its boiling point where N₂ flows through the neck of the Dewar. No theoretical procedure to predict the exit temperature of the N₂ gas and cooling mechanism of regenerator part. We have used ANSYS Fluent software to determine the temperature profile of nitrogen precooling. From the outside the regenerator is SS casing of 102 mm in length and OD of 96 mm. At inside the regenerator is inside a G10 displacer with a gap of few microns between the SS wall and displacer. This gap of few microns is filled by the working Helium gas. We have assumed 2-D axisymmetric model of cryocooler cold head with Dewar for studying temperature profile. Constraint temperatures and heat transfer coefficient of regenerator part were used as an input for boundary condition along the fluid entrance. For outside Dewar wall, adiabatic conditions were assumed. For this modeling, temperature profile with respect to distance of the cold head from regenerator part to bottom cold head has been found out by running the cryocooler in vacuum condition and at no load condition. Temperature profile with respect to distance of the cold head from regenerator part to bottom cold head has been shown in fig.8.14. The cooling curve of AL300 GM Cryocooler has been drawn in vacuum condition to get the initial temperature at the different position of GM Cryocooler, which is shown in fig.8.14. With the help of graph in fig.8.14, we have drawn Heat transfer coefficient of GM Cryocooler at different position of regenerator part that is shown in fig.8.16. For this, we have considered 5mm distance along the cryocooler to calculate the heat transfer area as well as heat transfer co-efficient of cryocooler cold head part and regenerator part. The actual position of sensors on GM Cryocooler is shown in fig.8.15.

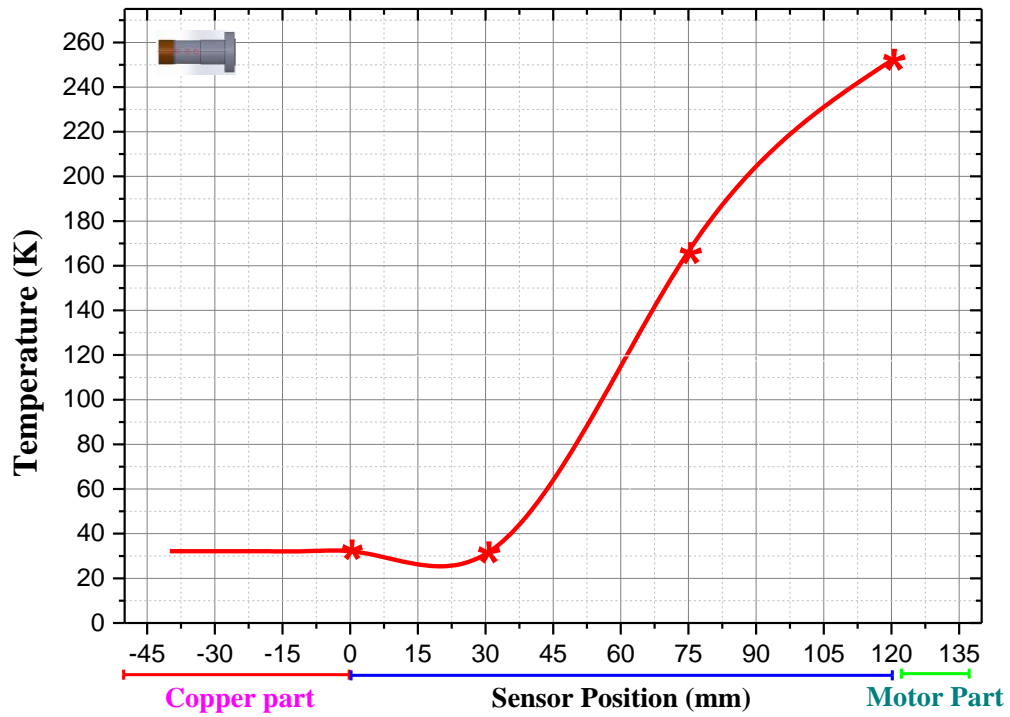


Fig.8.14- Cooling curve of AL300 GM Cryocooler in vacuum condition.

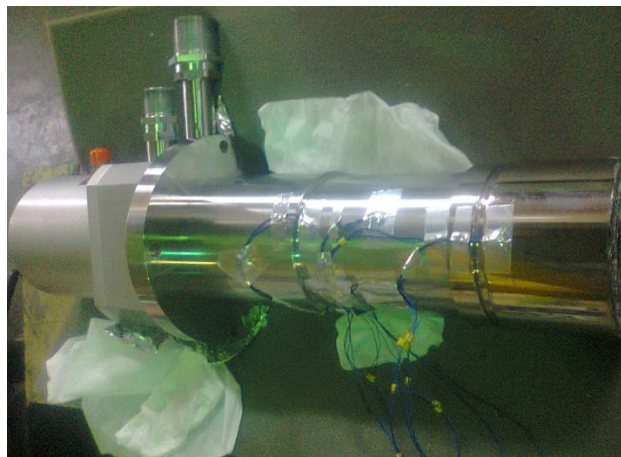


Fig.8.15- Sensors position on GM Cryocooler for generating cooling curve in vacuum condition

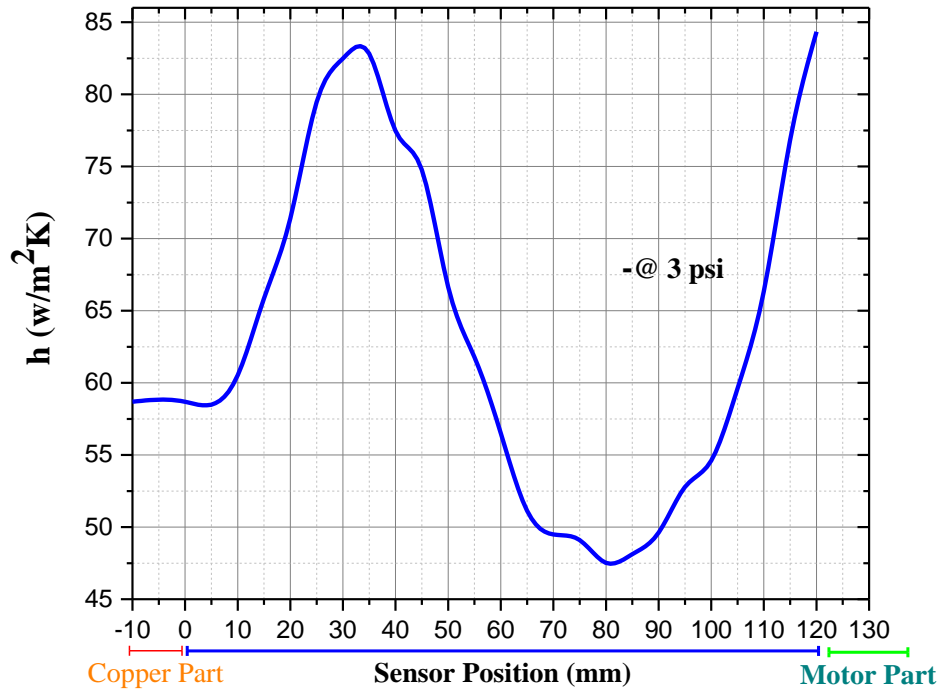


Fig.8.16: Heat transfer coefficient graph at different position of regenerator of AL300 GM Cryocooler

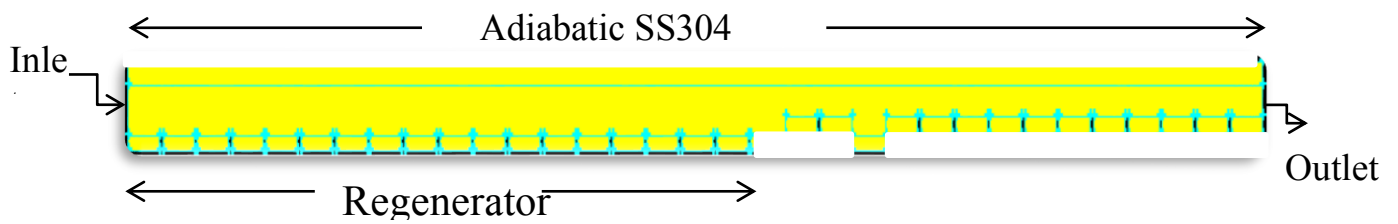


Fig.8.17: 2-D axisymmetric mesh model of the cold head with Dewar neck for CFD analysis.

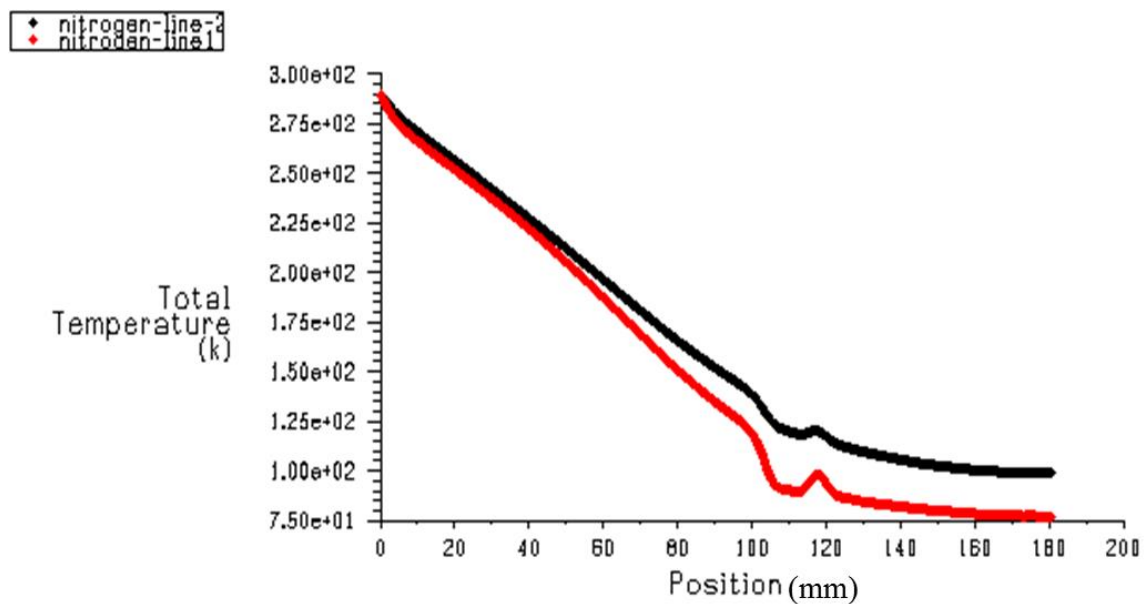
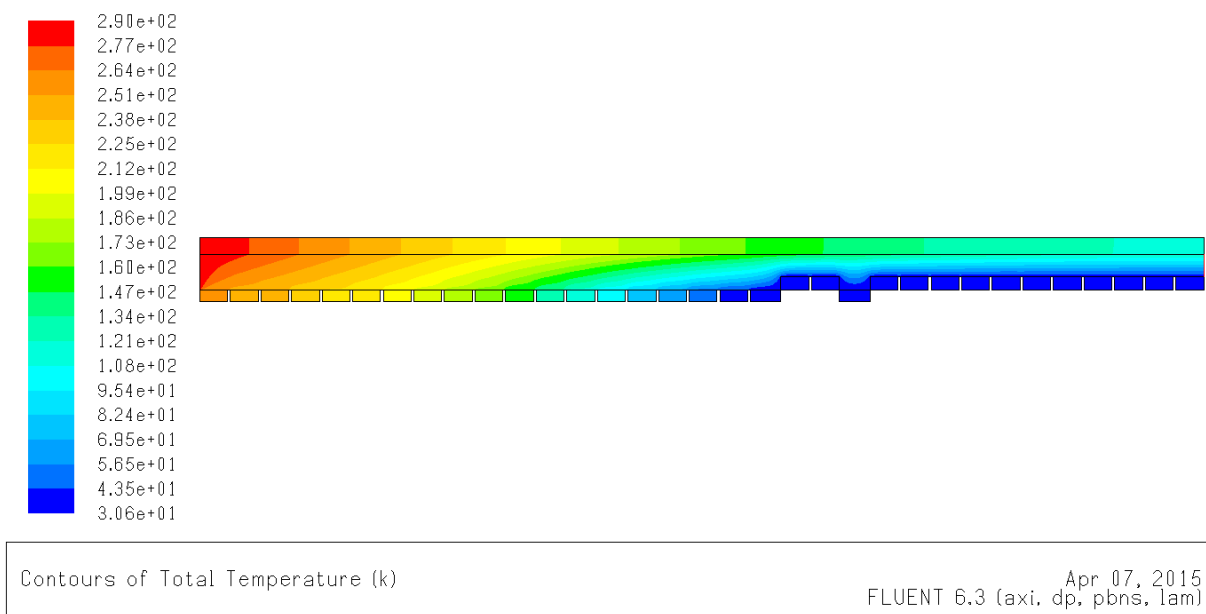


Fig.8.18: Temperature contour and Temperature Profile of the nitrogen gas through regenerator with 4mm annular gap.

Area-Weighted Average Total Temperature (k)	
n2_outlet	77.268661

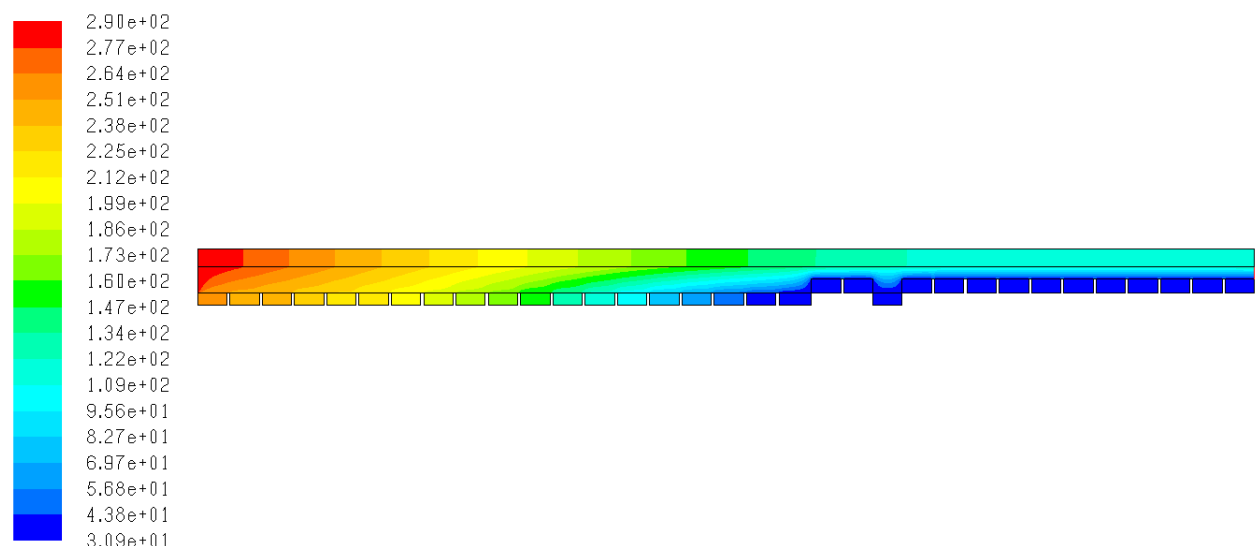
Fig.8.19: Flux report of the simulation for 4mm annular gap.

The above simulation was done with the actual geometry. The annular gap between cryocooler bottom cold head and the neck portion of SS304 pipe is 4 mm in this case. The output temperature obtained in ANSYS simulation is matched with the practical data. This 2-D simulation was done with a mass flow rate of 0.66 g/s and vessel operating pressure of 3 psi that gives us the temperature of the fluid at the exit of Cold Head as 77.268 K. The inlet temperature is taken as 290K. The property of fluid and solid has been entered at least for 10 points from 300K to 77K.

Now reduce the gap between the cold head and the SS304 pipe by reducing the OD and ID of the pipe with the same length. If the cross-sectional area of annular space is reduced turbulence will increase and hence heat transfer between the regenerator, and the fluid will increase. If the cross-sectional area of neck will decrease for the same length then it will reduce the conduction load coming on the cryogen reservoir.

Example:

Neck with cold head with 2 mm annular gap.



Contours of Total Temperature (k)

Apr 07, 2015
FLUENT 6.3 (axi, dp, pbns, lam)

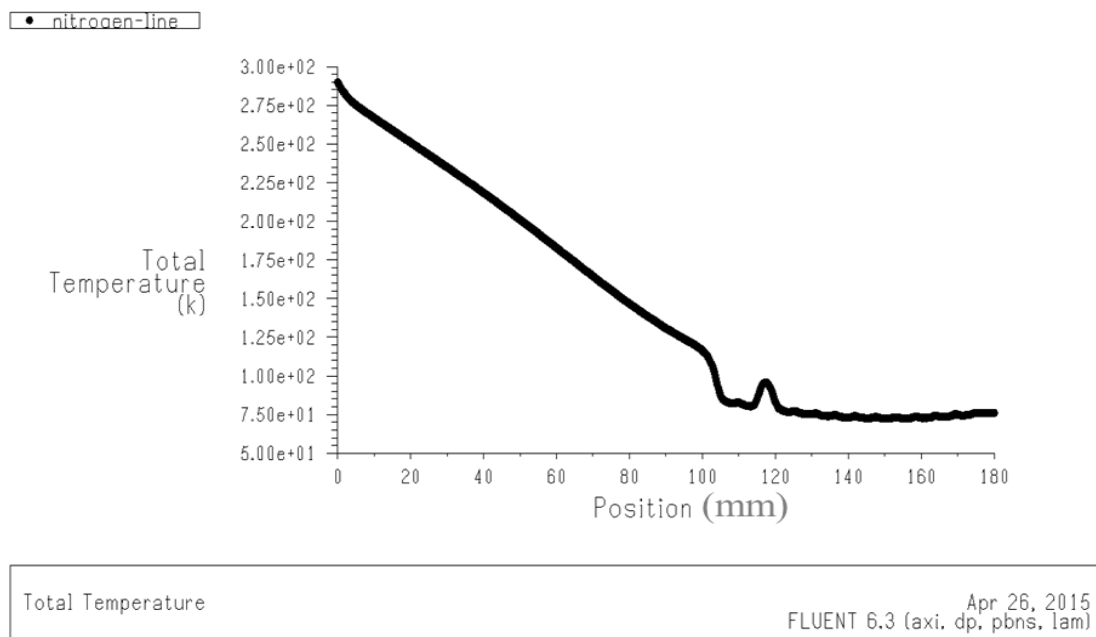


Fig.8.20: Temperature contour and Temperature Profile of the nitrogen fluid through regenerator with 2mm annular gap.

Area-Weighted Average Total Temperature		(K)
n2_out	76.484489	

Fig.8.21: Flux report of the simulation for 2 mm annular gap.

The output temperature reduced to 76.48 K for the case of 2mm annular gap but in previous case it was 77.26 K. This shows that by reducing the annular cross-sectional area, the precooling effect by regenerator part of cold head and temperature can be increased which will increase the production rate of nitrogen. Hence, annular gap must be kept minimum as possible to increase the production rate by using more precooling effect of the regenerator part of cold head. This also has an advantage of reducing the conduction load coming through the neck of Dewar.

Table No. 8.4: Enthalpy and temperature for different geometry.

Annular Gap (in mm)	$\dot{m}(\text{kg/s})$	Nitrogen Inlet Temperature (K)	Nitrogen Exit Temperature (K)	Enthalpy Removed (J/g)
4.1	6.6E-4	290	77.268	224.16
2.5	6.6E-4	290	76.48	225.09

CHAPTER 9

CONCLUSION

CHAPTER 9

CONCLUSION

Our new design in case of Helium liquefaction system exhibits higher liquefaction efficiency [l/day/kW] than the present best liquefier based on a pulse tube cold head, exploiting solely the cooling power of the cold head. It is even competitive with more complex devices, which involve either extra cooling with liquid nitrogen or an additional Joule–Thomson stage. The technological differences of GM and pulse tube cryocoolers raised questions on the suitability of GM cryocoolers for helium liquefaction. Due to the high thermal resistance between the incoming gas and the regenerative material, a typical GM type cooler with 1.5 W may not provide liquefaction rate >10 lit./day. However, this argument fails to be true – our present results show that one may use the temperature gradient between the first and the second stage of the GM cold head for efficient precooling of the incoming gas. We have achieved 20 lit./day liquefaction rate of helium with the help of GM cryocooler. An experimental dewar of 2 Litres capacity was designed and developed for liquid helium production in IUAC, New Delhi. Unique designs of the helium liquefaction system result in low cost, high reliability and high efficiency. These portable helium liquefaction systems can be used for the helium recovery and liquefaction from multiple cryostats on the site.

In case of a nitrogen liquefaction system, experimental runs with different scenarios were done to optimize the production rate of the setup. We have varied the cryostat pressure from 3 psi to 15 psi to increase the production rate. The production rate varies from 74 Ltr/ day to 80 Ltr/day was achieved at steady state in the experimental setup.

Three different type of temperature sensors were calibrated for both type of system and were placed in particular position in the experimental dewar and on the cold head to gather data for theoretical and analytical study of the setup.

REFERENCES

- [1] Mc Mahon H O and Gifford W E 1960, Adv. Cryog. Eng. 5, 354
- [2] Mikulin E I, Tarasov A A and Shkrebyonock M P 1984, Adv.Cryog. Eng. 29, 629
- [3] Wang, C., Helium liquefaction with a 4 K pulse tube cryocooler, Cryogenics, vol.41, no.7 (2001), pp.491-496.
- [4] Chao Wang, John G. Hartnett, A vibration free cryostat using pulse tube cryocooler, Cryogenics, Volume 50,no. 5 (2010), pp. 336-341
- [5] Patent no US20130014517 A1, Liquefier with pressure-controlled liquefaction chamber, Jost Diederichs, Ronald Sager, Quantum Design Inc., 2014
- [6] Cryogenic systems by Barron, R.F. (1985).
- [7] Vacuum Technology And Process Applications by Prof. V.V.Rao.
- [8] Gas Liquefier by Chao Wang, United States Patent Application Publication.
- [9] Small Scale Helium Liquefaction Systems by Chao Wang, 25th International Conference on Low-Temperature Physics (LT25).
- [10] Vapor Precooling in a Pulse Tube Liquefier by E.D. Marquardt, Ray Radebaugh, and A.P. Peskin Presented at the 11th International Cryocooler Conference June 20-22, 2000 Keystone, Co.
- [11] Cryogenic Material Properties Database by E.D. Marquardt, J.P. Le, and Ray Radebaugh, National Institute of Standards and Technology.
- [12] The Gifford-Mcmahon Cycle By W.E.Gifford (1965) Cryogenic Engineering Conference.
- [13] www.cryomech.com
- [14] Sumitomo Heavy Industries Limited.
- [15] Thummes G, Wang C, Heiden C. Small scale 4He liquefaction using a two-stage 4 K pulse tube cooler. Cryogenics 1998;38:337
- 14. Design and development of cryocooler based liquid nitrogen plant, Ashish Kumar, NIT ROURKELA.